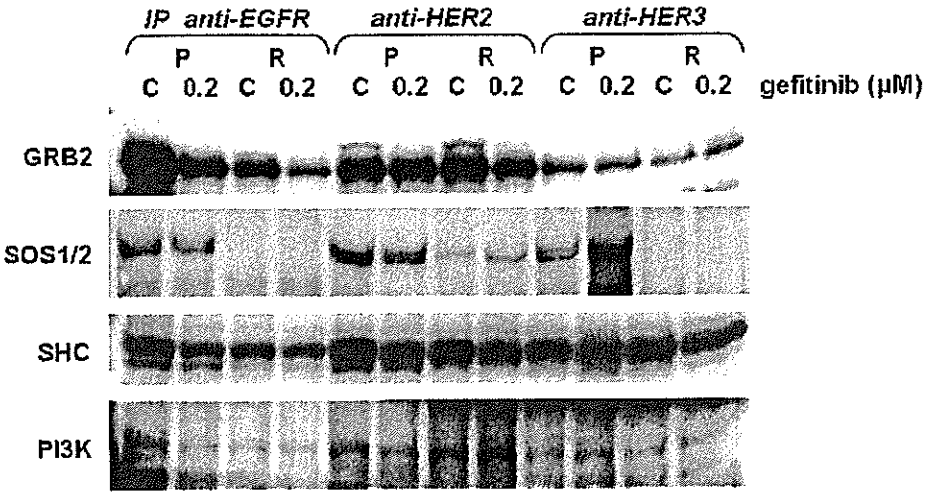

FIGURE 6 – Protein interaction between EGFR and its adaptor proteins. Cells (P: PC-9, R: PC-9/ZD) were exposed to 0 and 0.2 μM of gefitinib for 6 hr. The cells were lysed and immunoprecipitated with ant-EGFR, anti-HER2, and anti-HER3 antibodies, and the amounts of the Grb2, SOS1/2, SHC and PI3K precipitated were monitored by immunoblotting with their specific Abs.

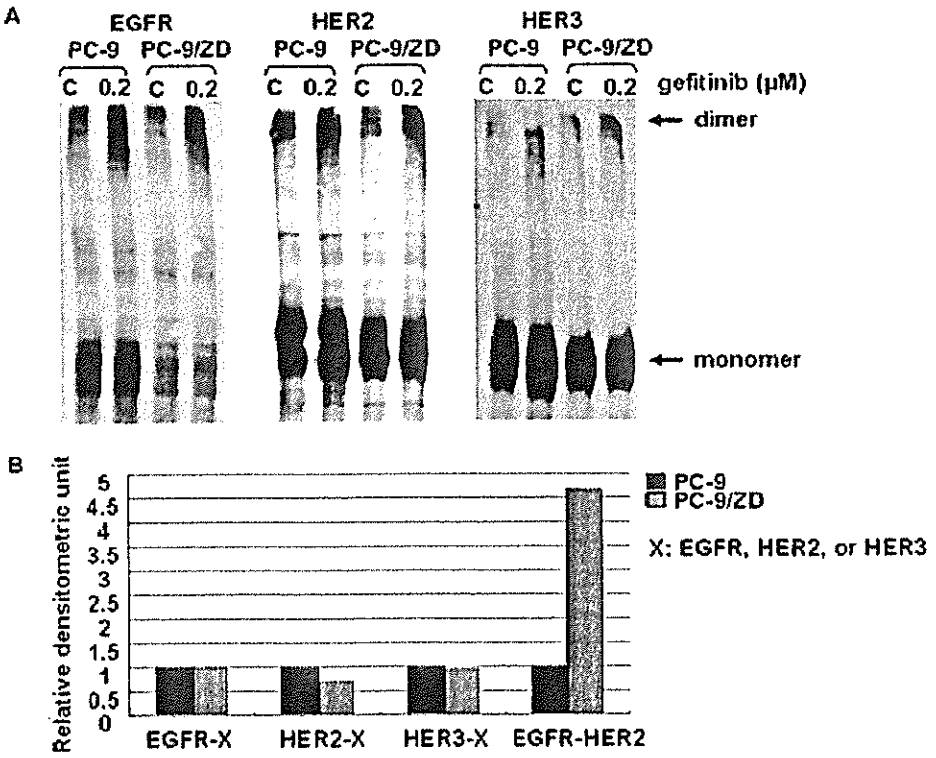

FIGURE 7 – Chemical cross-linking of PC-9 and PC-9/ZD cells. (*a*) After 6 hr exposure to 1.5 mM bis (sulfosuccinimidyl) substrate dissolved in PBS as indicated in Material and Methods. The cross-linking reaction was quenched and the cell lysates were prepared and subjected to immunoblot analysis of EGFR, HER2 and HER3. (*b*) Ratio of dimmers formed by PC-9 cells to those by PC-9/ZD cells in the absence of gefitinib. The density of the bands in (*a*) for EGFR-X, HER2-X and HER3-X were quantified densitometrically. The ratio of EGFR-HER2 was calculated by the band density obtained in Figure 5*a*. X = EGFR, HER2 or HER3.

Discussion

Interest in resistance to target-based therapy (TBT) has been growing ever since clinical efficacy was first demonstrated.[11–13] Although CML patients respond to STI-571 well at first, most patients eventually relapse in the late stage of the disease.[25–27] It has been reported that some patients in whom treatment with gefitinib is effective at first, ultimately become refractory.[30] Resistance is likely to remain a hurdle that limits the long-term effectiveness of TBT. PC-9 had a deletion mutation within the kinase domain of *EGFR* and is highly sensitive. These characters are similar to those of NSCLC with clinical responsiveness to gefitinib. Analyzing the mechanism of resistance of PC-9/ZD subline might be clinically meaningful.

The mechanism of drug resistance is thought to be multifactorial. Because the growth-inhibitory assay in our present study showed no cross resistance to a variety of cytotoxic agents, the mechanism of the resistance differs from the mechanism of multidrug resistance patterns. Although expression of BCRP, one of the multidrug-resistance-related proteins has been reported to contribute to the resistance to gefitinib,[31] expression of *BCRP* mRNA is observed only in PC-9 cells (data not shown). Although mutations in the ATP-binding pocket of *BCR-ABL* gene have been identified recently in cells from CML patients who were refractory to STI-571 treatment or relapse,[25–27] there have been no reports of any such mutations for gefitinib resistance. PC-9/ZD also became refractory to gefitinib without secondary mutation in *EGFR* cDNA. These suggest the possibility of refractory tumor after treatment of gefitinib including this kind of phenotype.

There is no significant difference in expression level of EGFR between PC-9 and PC-9/ZD. Does the antitumor effect of gefitinib

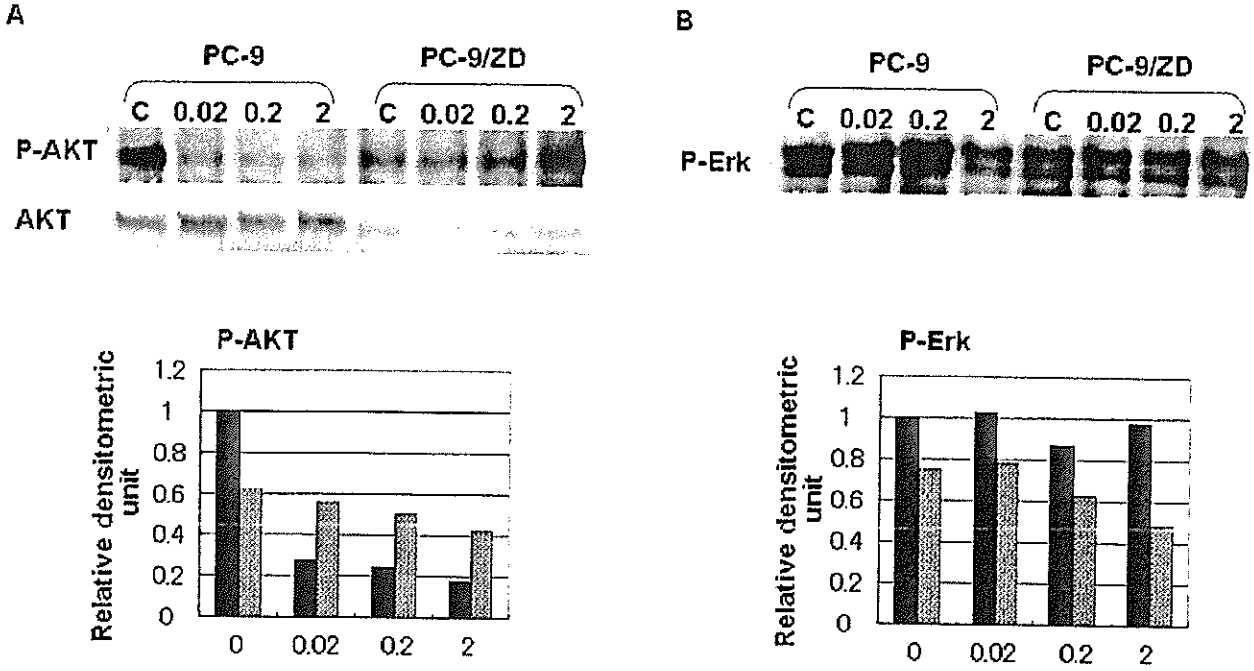

FIGURE 8 – Effect of gefitinib on the MAPK and AKT pathway. Cells were placed in medium containing 0, 0.02, 0.2 or 2 μM of gefitinib for 6 hr and harvested in EBC buffer. Total cellular lysates were separated on SDS-PAGE, transferred to a membrane and blotted with (*a*) anti-phospho-AKT (Ser473) and (*b*) anti-phospho-Erk (p44/42) antibodies. The expression levels are shown in a graph.

require EGFR expression? Naruse *et al.*[32] suggested that the high sensitivity of K562/TPA to gefitinib is due to acquired EGFR expression. In their study autophosphorylation of EGFR in K562/TPA cells was inhibited by 0.01 μM gefitinib, and the IC_{50}-value of gefitinib in parental K562 cells, which do not express EGFR, was approximately 400-fold higher than that in the K562/TPA subline. Furthermore, most patients who responded to gefitinib therapy have *EGFR* mutation in lung tumor.[18,19] These findings suggest strongly that gefitinib exerts its antitumor effect through an action on EGFR. Our present study showed similar EGFR expression and autophosphorylation levels in PC-9 and PC-9/ZD cells. The inhibitory effect of gefitinib on phosphorylation of EGFR is different. PC-9/ZD did not show cross-resistance to the specific EGFR TK inhibitors RG-14620 and Lavendustin A in an MTT assay, nor did inhibit the phosphorylation of EGFR at the cellular level (data not shown). Paez *et al.*[18] reported that phosphorylation of EGFR in gefitinib-resistant cell lines was inhibited only when gefitinib was present at high concentration. These findings suggest that the difference in the inhibitory-effect on EGFR phosphorylation may determine the efficacy of the drug.

The inhibitory effect of gefitinib on EGFR phosphorylation is not significant in PC-9/ZD cells despite the absence of differences in the sequences of *EGFR*, *HER2*, and *HER3*. There are several possible explanations for the difference in inhibitory effect. First, the avidity of gefitinib for the ATP-binding site of EGFR may be decreased in PC-9/ZD cells due to a protein-protein interaction, *i.e.*, EGFR and a certain protein prevent gefitinib from binding to EGFR. Second, a change in the activity of specific protein-tyrosine kinase or phosphatase of EGFR in PC-9/ZD cells, especially after exposure to gefitinib, may result in resistance to inhibition of EGFR phosphorylation. The phosphorylation level is maintained in exquisite balance by the reciprocal activities of kinase and phosphatase,[33,34] and Wu reported that phosphatase plays a role in STI571-resistance.[35] Third, increased heterodimer formation by EGFR with other members of the HER family results in the limited inhibition. Heterodimer formation is increased in PC-9/ZD cells under basal conditions, and no increase in formation was observed after exposure to gefitinib, although marked heterodimer induction was observed in PC-9 cells. Calculations in *in vitro* studies have shown that the IC_{50}-value for inhibition of the tyrosine kinase activity of EGFR is 0.023–0.079 μM, whereas the IC_{50}-value for inhibition of HER2 is 100-fold higher.[36] We estimate that the inhibitory effect of gefitinib depends on the ratio of homodimer formation to heterodimer formation, and the heterodimer may be one of the routes of escape from the action of gefitinib.

Signal transduction by the HER family member is mediated by 2 major pathways, the MAPK signaling pathway and the AKT signaling pathway, which regulate cell proliferation and survival. Because phosphorylated AKT was inhibited completely by gefitinib in PC-9 cells, but inhibition of phosphorylated MAPK was not significant, inhibition of the AKT pathway may be more important to cell sensitivity than inhibition of MAPK. Moasser *et al.*[37] reported consistent results, showing that downregulation of AKT activity is predominantly seen in tumors that are sensitive to gefitinib. The phosphorylation of AKT and MAPK was not inhibited significantly by gefitinib in PC-9/ZD cells. This finding might be attributable to inactivation of Tyr 1068-GRB2-SOS-mediated signaling.

Based on the results of this comparative study, EGFR-GRB2-SOS complex formation, phosphorylation of Tyr1068, the ratio of the amount of homodimer formation to heterodimer formation, and the AKT signaling pathway are possible predictive biomarkers for gefitinib sensitivity. As a different approach, we are now looking for the genes associated with gefitinib resistance in PC-9/ZD cells compared to PC-9 cells by subtractive cloning.

Acknowledgements

'Iressa' is a trademark of the AstraZeneca group of companies.

References

1. Socinski MA. Addressing the optimal duration of therapy in advanced, metastatic non-small-cell lung cancer. In: Perry MC, eds. American Society of Clinical Oncology Educational Book. Alexandria: Lisa Greaves. 2003;144–52.
2. Nicholson RI, Gee JM, Harper ME. EGFR and cancer prognosis. Eur J Cancer 2001;37:S9–15.
3. Mendelsohn J, Baselga J. The EGF receptor family as targets for cancer therapy. Oncogene 2000:19:6550–65.
4. Salmon DS, Brandt R, Ciardiello F, Normanno N. Epidermal growth factor-related peptides and their receptors in human malignancies. Crit Rev Oncol Hematol 1995;19:182–232.
5. Fox SB, Smith K, Hollyer J, Greenall M, Hastrich D, Harris AL. The epidermal growth factor receptor as a prognostic marker: result of 370 patients and review of 3009 patients. Breast Cancer Res Treat 1994;29:41–99.
6. Dassonville O, Formento JL, Francoual M, Ramaioli A, Santini J, Schneider M, Demard F. Expression of epidermal growth factor receptor and survival in upper aerodigestive tract cancer. J Clin Oncol 1993;11:1873–8.
7. Sainsbury JR, Farndon JR, Needham GK, Malcolm AJ, Harris AL. Epidermal-growth-factor receptor status as predictor of early recurrence of and death from breast cancer. Lancet 1987;1:1398–402.
8. Scambia G, Benedetti-Panici P, Ferrandina G, Distefano M, Salerno G, Romanini ME, Fagotti A, Mancuso S. Epidermal growth factor, oestrogen and progesterone receptor expression in primary ovarian cancer: correlation with clinical outcome and response to chemotherapy. Br J Cancer 1995;72:361–6.
9. Veale D, Ashcroft T, Marsh C, Gibson GJ, Harris AL. Epidermal growth factor receptors in non-small cell lung cancer. Br J Cancer 1987:55:513–6.
10. Veale D, Kerr N, Gibson GJ, Kelly PJ, Harris AL. The relationship of quantitative epidermal growth factor receptor expression in non-small cell lung cancer to long term survival. Br J Cancer 1993;68:162–5.
11. Druker BJ, Talpaz M, Resta DJ, Peng B, Buchdunger E, Ford JM, Lydon NB, Kantarjian H, Capdeville R, Ohno-Jones S, Sawyers CL. Efficacy and safety of a specific inhibitor of the BCR-ABL tyrosine kinase in chronic myeloid leukemia. N Engl J Med 2001;344: 1031–7.
12. Druker BJ, Sawyers CL, Kantarjian H, Resta DJ, Reese SF, Ford JM, Capdeville R, Talpaz M. Activity of a specific inhibitor of the BCR-ABL tyrosine kinase in the blast crisis of chronic myeloid leukemia and acute lymphoblastic leukemia with the Philadelphia chromosome. N Engl J Med 2001;344:1038–42.
13. Joensuu H, Roberts PJ, Sarlomo-Rikala M, Andersson LC, Tervahartiala P, Tuveson D, Silberman S, Capdeville R, Dimitrijevic S, Druker B, Demetri GD. Effect of the tyrosine kinase inhibitor STI571 in a patient with a metastatic gastrointestinal stromal tumor. N Engl J Med 2001;344:1052–6.
14. Fukuoka M, Yano S, Giaccone G, Tamura T, Nakagawa K, Douillard JY, Nishiwaki Y, Vansteenkiste J, Kudoh S, Rischin D, Eek R, Horai T, et al. Multi-institutional randomized phase II trial of gefitinib for previously treated patients with advanced non-small-cell lung cancer. J Clin Oncol 2003;21:2227–9.
15. Kris MG, Natale RB, Herbst RS, Lynch TJ Jr, Prager D, Belani CP, Schiller JH, Kelly K, Spiridonidis H, Sandler A, Albain KS, Cella D, et al. Efficacy of gefitinib, an inhibitor of the epidermal growth factor receptor tyrosine kinase, in symptomatic patients with non-small cell lung cancer: a randomized trial. JAMA 2003;290:2149–58.
16. Giaccone G, Herbst RS, Manegold C, Scagliotti G, Rosell R, Miller V, Natale RB, Schiller JH, Von Pawel J, Pluzanska A, Gatzemeier U, Grous J, *et al*. Gefitinib in combination with gemcitabine and cisplatin in advanced non-small-cell lung cancer: a phase III trial—INTACT 1. J Clin Oncol 2004:22: 777–84.
17. Miller VA, Johnson DH, Krug LM, Pizzo B, Tyson L, Perez W, Krozely P, Sandler A, Carbone D, Heelan RT, Kris MG, Smith R, et al. Pilot trial of the epidermal growth factor receptor tyrosine kinase inhibitor gefitinib plus carboplatin and paclitaxel in patients with stage IIIB or IV non-small-cell lung cancer. J Clin Oncol 2003;21: 2094–100.
18. Paez JG, Janne PA, Lee JC, Tracy S, Greulich H, Gabriel S, Herman P, Kaye FJ, Lindeman N, Boggon TJ, Naoki K, Sasaki H, et al. EGFR mutations in lung cancer: correlation with clinical response to gefitinib therapy. Science 2004;304:1497–500.
19. Lynch TJ, Bell DW, Sordella R, Gurubhagavatula S, Okimoto RA, Brannigan BW, Harris PL, Haserlat SM, Supko JG, Haluska FG, Louis DN, Christiani DC, et al. Activating mutations in the epidermal growth factor receptor underlying responsiveness of non-small-cell lung cancer to gefitinib. N Engl J Med 2004;350: 2191–3.
20. Pao W, Miller V, Zakowski M, Doherty J, Politi K, Sarkaria I, Singh B, Heelan R, Rusch V, Fulton L, Mardis E, Kupfer D, et al. EGF receptor gene mutations are common in lung cancers from "never smokers" and are associated with sensitivity of tumors to gefitinib and erlotinib. Proc Natl Acad Sci USA 2004: 101:13306–11.
21. Nomori H, Saijo N, Fujita J, Hyoi M, Sasaki Y, Shimizu E, Kanzawa F, Inomata M, Hoshi A. Detection of NK activity and antibody-dependent cellular cytotoxicity of lymphocytes by human tumor clonogenic assay—its correlation with the 51Cr-release assay. Int J Cancer 1985;35:449–55.
22. Mosmann T. Rapid colorimetric assay for cellular growth and survival: application to proliferation and cytotoxicity assays. J Immunol Meth 1983;65:55–63.
23. Arteaga CL, Ramsey TT, Shawver LK, Guyer CA. Unliganded epidermal growth factor receptor dimerization induced by direct interaction of quinazolines with ATP binding site. J Biol Chem 1998:273:18623–32.
24. Gorre ME, Mohammed M, Ellwood K, Hsu N, Paquette R, Rao PN, Sawyers CL. Clinical resistance to STI-571 cancer therapy caused by BCR-ABL gene mutation or amplification. Science 2001:293:876–80.
25. Von Bubnoff N. BCR-ABL gene mutation in relation to clinical resistance Lancet 2002;356:487–91.
26. McCormick F. New-age drug meets resistance. Nature 2001;412: 281–2.
27. Ricci C, Scappini B, Divoky V, Onida F, Verstovsek S, Kantarjian HM, Beran M. Mutation in the ATP binding pocket of the ABL kinase domain in and STI571-resistant BCR/ABL-positive cell line. Cancer Res 2002;62:5995–8.
28. Laffargue M, Raynal P, Yart A, Peres C, Wetzker R, Roche S, Payrastre B, Chap H. An epidermal growth factor receptor/Gab1 signaling pathway is required for activation of phosphoinositide 3-kinase by lysophosphatidic acid. J Biol Chem 1999;274:32835–41.
29. Rodriguez-Viciana P, Warne PH, Dhand R, Vanhaesebroeck B, Gout I, Fry MJ, Waterfield MD, Downward J. Phosphatidylinositol-3-OH kinase as a direct target of Ras. Nature 1994;370:527–32.
30. Kurata T, Tamura K, Kaneda H, Nogami T, Uejima H, Asai Go G, Nakagawa K, Fukuoka M. Effect of re-treatment with gefitinib ('Iressa', ZD1839) after acquisition of resistance. Ann Oncol 2004;15:173–4.
31. Yanase K, Tsukahara S, Asada S, Ishikawa E, Imai Y, Sugimoto Y. Gefitinib reverses breast cancer resistence protein-mediated drug resistence. Mol Cancer Ther 2004;3:1119–25.
32. Naruse I, Ohmori T, Ao Y, Fukumoto H, Kuroki T, Mori M, Saijo N, Nishio K. Antitumor activity of the selective epidermal growth factor receptor- tyrosine kinase inhibitor (EGFR-TKI) Iressatm (ZD1839) in a EGFR-expressing multidrug resistant cell line in vitro and in vivo. Int J Cancer 2002;98:310–5.
33. Reynolds AR, Tischer C, Verveer PJ, Rocks O, Bastiaens PIH. EGFR activation coupled to inhibition of tyrosine phosphatases causes lateral signal propagation. Nat Cell Biol 2003;5:447–53.
34. Haj FG, Markova B, Klaman LD, Bohmer FD, Neel BG. Regulation of receptor tyrosine kinase signaling by protein tyrosine phosphatase-1B. J Biol Chem 2003;278:739–44.
35. Wu JY, Talpaz M, Donato NJ. Tyrosine kinases and phosphatase play a role in STI571-mediate apoptosis of chronic myelogenous leukemia cells. Proc Am Assoc Cancer Res 2003;44(2nd ed.) 205:(Abstract 1016).
36. Wakeling AE, Guy SP, Woodburn JR, Ashton SE, Curry BJ, Barker AJ, Gibson KH. ZD1839 (Iressa): an orally active inhibitor of epidermal growth factor signaling with potential for cancer therapy. Cancer Res 2002;62:5749–54.
37. Mousser MM, Basso A, Averbuch SD, Rosen N. The tyrosine kinase inhibitor ZD1839 ("Iressa") inhibits HER2-driven signaling and suppresses the growth of HER2-overexpressing tumor cells. Cancer Res 2001;61:7184–8.

Int. J. Cancer: 108, 679–685 (2004)

Publication of the International Union Against Cancer

hnRNP L ENHANCES SENSITIVITY OF THE CELLS TO KW-2189

Fumiko TAGUCHI[1,3], Hitoshi KUSABA[1], Akira ASAI[4], Yasuo IWAMOTO[1], Keiichi YANO[4], Hirofumi NAKANO[4], Tamio MIZUKAMI[4], Nagahiro SAIJO[2], Harubumi KATO[3] and Kazuto NISHIO[1]*

[1]*Pharmacology Division, National Cancer Center Research Institute, Tokyo, Japan*
[2]*Medical Oncology Division, National Cancer Center Hospital, Tokyo, Japan*
[3]*Department of Surgery, Tokyo Medical University, Tokyo, Japan*
[4]*Tokyo Research Laboratories, Kyowa Hakko Kogyo Co. Ltd, Tokyo, Japan*

Heterogeneous nuclear ribonucleoproteins (hnRNPs) are involved in several RNA-related biological processes. We demonstrated hnRNP L as a candidate protein of DARP (duocarmycin-DNA adduct recognizing protein) by gel shift assay and amino acid sequencing. Stable transfectants of hnRNP L showed high sensitivity of the cells to the growth inhibitory effect of KW-2189, a duocarmycin derivative *in vitro*. Immunostaining of hnRNP L demonstrated differential intracellular localization of hnRNP L among human lung cancer cell lines. A transfection study using a series of deletion mutants of hnRNP L fused to indicated that the N-terminal portions of RRM(RNA recognition motif)1, RRM3 and RRM2 are involved in localization of hnRNP L. We identified sequences in these portions that have high homology with the sequences of known NLS (nuclear localization signal) and NES (nuclear export signal). hnRNP L is a factor that determines the sensitivities of cancer cells to the minor groove binder, and overexpression and differential intracellular localization of hnRNP L are involved in its function in lung cancer.

Key words: *hnRNP L; KW-2189; duocarmycin; minor groove binder; nuclear localization signal*

Heterogeneous nuclear ribonucleoproteins (hnRNPs) participate in a variety of processes involving RNA, including transcription, splicing, processing, translation and turnover, and there are approximately 20 major members of the hnRNP family.[1] High expression of some of these have been reported in several human malignant tumors and interest in the action of these proteins in malignancies has been growing.[2,3] HnRNP L is 68 kDa protein with 4 RNA recognition motifs (RRM). There have been several interesting reports demonstrating that cytoplasmic hnRNP L specifically interacts with VEGF mRNA in hypoxic cells *in vivo*, regulates VEGF mRNA stability[4] and binds in a sequence-specific manner to a *cis*-acting RNA sequence element that enables intron-independent gene expression.[5] The role of hnRNP L, however, still requires further study.

KW-2189 is a water-soluble derivative of antitumor antibiotic duocarmycin (DUM),[6–8] and DUM and its derivatives have been reported to exert their anti-tumor activity through covalent binding to the DNA minor groove and inhibition of DNA synthesis. We identified previously a nuclear protein DARP (duocarmycin-DNA adduct recognizing protein) in human cervical carcinoma HeLa S3 cells.[9] We purified the DARP from nuclear extract of HeLa S3 and its amino acid sequence was identical to hnRNP L. We investigated this, particularly in cancer cells.

MATERIAL AND METHODS

Cell cultures and reagents

Human small cell lung cancer cell lines SBC-3 and H69, human non-small cell lung cancer cell lines PC-14, and their respective cisplatin-resistant cell lines (SBC-3/CDDP, H69/CDDP,[10] and PC-14/CDDP[11]) were maintained in RPMI 1640 (Sigma, St. Louis, MO) supplemented with 10% heat-inactivated FBS (Gibco BRL, Gaithersburg, MD). Murine fibroblast cell line NIH3T3 and sublines (including cDNA transfectants) were cultured in DMEM (Nissui Pharmaceutical Co. Ltd., Tokyo, Japan) supplemented with 10% FBS. KW2189 was provided by Kyowa Hakko Kogyo Co., Ltd. A monoclonal antibody specific for hnRNP L (4D11) was generously provided by Dr. G. Dreyfuss (University of Pennsylvania, Philadelphia).

Cell extracts

Cells were washed twice with cold PBS and lysed in buffer (10 mM Tris-HCl pH 7.8, 1% Nonidet P-40, 0.15 M NaCl, 1 mM EDTA, 10 μg/ml aprotinin, 0.5 μg/ml leupeptin, 1 mM phenylmethane-sulfonyl fluoride [PMSF], 1 tablet/50 ml φgrComplete™ and 10% glycerol) for 60 min on ice. The lysates were centrifuged at 8,000*g* for 20 min, and supernatants were obtained as total protein. Protein concentration was measured by bicinchoninic acid protein assay (Pierce, Rockford, IL).

SBC-3, PC-14 and H69 cells were lysed in buffer A containing 10 mM HEPES-KOH (pH 7.9), 10 mM KCl, 0.1 mM EDTA-NaOH (pH 8.0), 0.1 mM ethyleneglycol bis(2-aminoethyl ether) tetraacetic acid (EGTA), 1 mM dithiothreitol (DTT), 0.5 mM PMSF, 1 mM aprotinin, and leupeptin. Nonidet P-40 (final concentration 0.5%) was added after allowing to stand on ice for 15 min. The supernatant obtained by centrifugation at 7,000*g* for 30 sec after standing on ice for 5 min was collected as the cytoplasmic fraction. The pellet was resuspended with buffer A containing 0.25 M sucrose, and after buffer B′ (buffer A containing 0.6 M sucrose) was added, the solution was centrifuged at 5,000*g* for 1 min at 4°C. The nuclei, which were contained in the pellet, were sonicated in buffer C containing 20 mM HEPES-KOH (pH 7.9), 0.4 M NaCl, 1 mM EDTA-NaOH (pH 8.0), 1 mM EGTA, 1 mM DTT and 1 mM PMSF, and then rocked at 4°C for 30 min and centrifuged at 8,000*g* for 10 min. The supernatant was used as the nuclear fraction. The nuclear protein content was adjusted to 5 μg per well, and the same volume of cytoplasmic protein was applied to the next well. The cytoplasmic and nuclear fractions were subjected to SDS-PAGE and Western blotting with anti-hnRNP L antibody.

Western blotting

An INSTA-Blot human tissues membrane (Imgenex, San Diego, CA), which contains 10 μg per lane of different human tissue lysates, was soaked in 100% methanol and then washed with TBST. After blocking the membrane in 5% skim milk in TBST for 1 hr at room temperature, it was probed with anti-hnRNP L antibody diluted (1:500) in TBST with 1% skim milk for 1 hr at

Fumiko Taguchi is a recipient of Research Resident Fellowship from the Foundation for Promotion of Cancer Research in Japan

*Correspondence to: Pharmacology Division, National Cancer Center Research Institute, 5-1-1 Tsukiji, Chuo-ku, Tokyo 104-0045, Japan. Fax: +81-3-3547-5185. E-mail: knishio@gan2.res.ncc.go.jp

Received 16 September 2002; Revised 25 August 2003; Accepted 12 September 2003

DOI 10.1002/ijc.11616

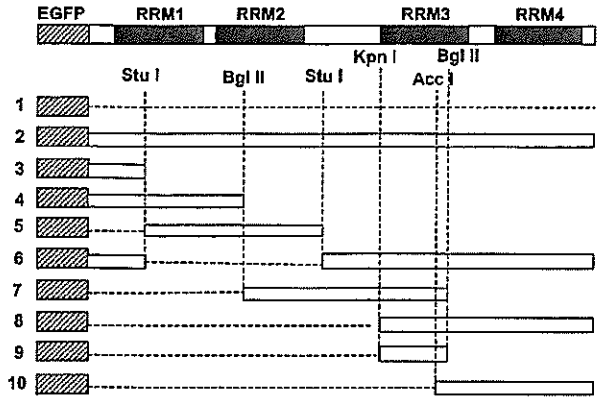

FIGURE 1 – Diagram of EGFP-hnRNP L deletion mutants. Known motifs, RNA recognition motifs (RRMs) 1, 2, 3 and 4 are boxed. The dark gray box denotes EGFP. Ten plasmids containing various parts of hnRNP L were constructed. The restriction sites used to generate deletion mutants are indicated.

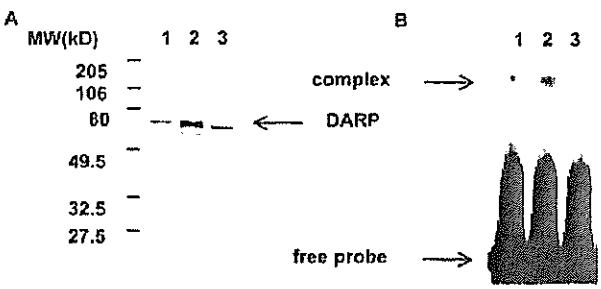

FIGURE 2 – Purification of DARP. (*a*) SDS-PAGE analysis of DEAE-sephacel fractions. *Lane 1*, 0.15 M KCl eluate; *Lane 2*, 0.2 M KCl eluate; *Lane 3*, 0.25 M KCl eluate. (*b*) Gel mobility shift assay of DEAE-sephacel fractions. *Lane 1*, 0.15 M KCl eluate; *Lane 2*, 0.2 M KCl eluate; *Lane 3*, 0.25 M KCl eluate. The oligonucleotides used as a probe contains the 5'-ATTA-3' sequence recognized by DUMSA (5'-GATC-CGGGATTACGATCGGGAGTCCCAGATTACGGCACCT-3'). The duplex oligonucleotides was incubated with each eluate after treatment with DUMSA as described in Material and Methods.

room temperature, washed 3 times in TBST, incubated with anti-mouse IgG horseradish peroxidase antibody diluted (1:5000) in TBST with 1% skim milk for 1 hr at room temperature, and then washed 3 times in TBST. The signal was visualized with ECL (Amersham Pharmacia Biotech UK Ltd., Buckinghamshire, England), and Hyperfilm-MP (Amersham) was exposed to it.

Purification of DARP and amino acid sequencing

Purification of DARP was conducted as described previously.[9] DARP was detected by its ability to bind to DUMSA (one of DUMs)-DNA adduct in gel shift assays. Nuclear and cytoplasmic extracts from HeLa S3 cells (ATCC: American Type Culture Collection) were prepared according to previously published procedures. For identification of the DARP band, the aliquot of this material was subjected to DEAE-sephacel column again, and eluted with 0.5M stepwise procedure (0.1–0.5 M KCl) to give the small amount of purified DARP. Protein concentrations were estimated using Bio-Rad protein assay and the quality of the each fraction was checked by CBB (Coomassie brilliant blue) or silver staining of SDS-polyacrylamide gels. For analysis of amino acids sequence of DARP about 2 μg of affinity purified DARP was separated by 12% SDS-PAGE. The 60 kDa protein band was excised and digested with lysyl endopeptidase (WAKO, Japan) in

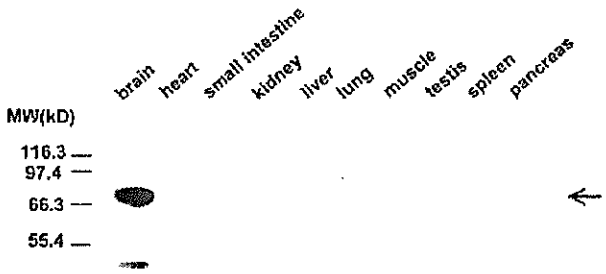

FIGURE 3 – Expression of hnRNP L in human tissues. Western blot analysis was carried out with anti-hnRNP L antibody. The membrane (INSTA-Blot) contains 10 μg per lane of different human tissue lysates. The arrow points to the hnRNP L protein.

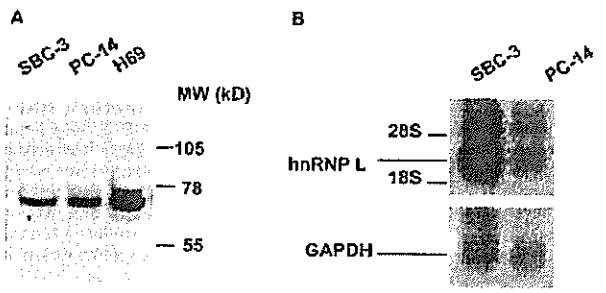

FIGURE 4 – Expression of hnRNP L in human lung cancer cell lines. (*a*) Cell lysates were prepared from 3 human lung cancer cell lines, separated with 7.5% SDS-PAGE, transferred to a membrane, and probed with anti-hnRNP L antibody. (*b*) Northern blotting was carried out with the 1030 bp fragment from hnRNP L cDNA as the probe.

0.1 M Tris-HCl (pH 9.0), 4 M urea at 37°C for 16 hr. The resulting peptides were isolated by reversed phase HPLC on a RPC C2/C18 column (Amersham Pharmacia Biotech, Sweden). The amino acid sequence was determined by automated Edman degradation using a PPSQ-10 protein sequencer (Shimadzu, Japan).

Gel mobility shift assay

Labeled oligonucleotide (1 μg) was incubated with cell extract (final protein concentration, 20 μg/μl) at 30°C for 30 min in the presence of 2 μg of poly[dIdC]poly[dIdC] and 1 μg of BSA, except where stated, in a final volume of 15 μl of 0.1 M KCl HEDG. Where indicated, drug modified or unmodified calf thymus DNA was added to the reactions. Samples were electrophoresed in 6% polyacrylamide gel, dried and scanned.

Stable transfectants

Total RNA was prepared from HeLa cells with ISOGEN (Nippon Gene, Tokyo, Japan), and 14–784 and 636—1718 fragments of hnRNP L (2033 bp) were obtained by reverse transcription-polymerase chain reaction (RT-PCR). The PCR products were cloned in PCR II, a TA cloning plasmid vector, and then coupled at the Bcl I site. Subsequently, a fragment including hnRNP L was digested from the plasmid with Not I, and it was informed into the Not I site of the pRc/CMV vector. After confirming its sequence, this expression vector, pRc/CMV, containing cDNA of hnRNP L, was transfected into NIH3T3 cells with the Lipofectin reagent (Gibco BRL) according to the manufacturer's instructions. After 48 hr incubation, 1.5 mg/ml of G418 (Sigma) was added. Cells resistant to neomycin were selected, and isolated by limiting dilution methods.

Northern blotting

Total RNAs were prepared from SBC-3, PC-14 and NIH3T3 cells, and the 10 stable transfectants described above with ISO-

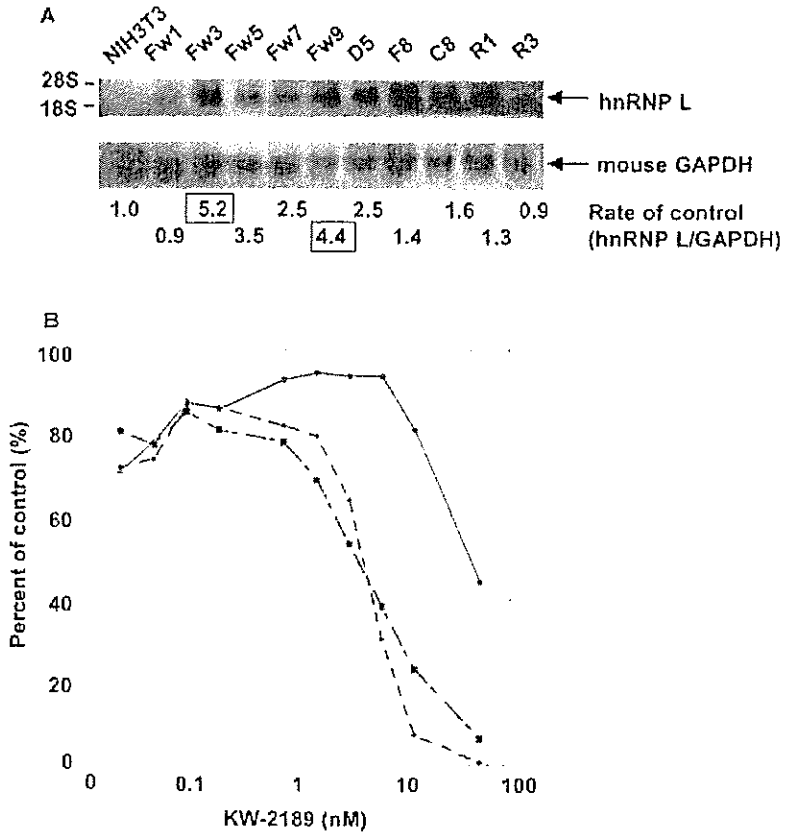

FIGURE 5 – Effect of hnRNP L on drug sensitivity. (*a*) Expression of hnRNP L mRNA in stable transfectants. Fw3 and Fw9 were chosen for the sensitivity tests. (*b*) MTT assay (KW-2189). C4 mock (●), Fw3 (■), Fw9 (□).

GEN reagent. RNA (12 μg) was electrophoresed and transferred to a positively charged nylon membrane (Hybond-N+). The 1030 bp fragment of hnRNP L cDNA was labeled with [α^{32}P]-dCTP by using the Rediprime II random primer labeling system (Amersham) and was used as a probe. The membrane was hybridized at 42°C overnight for blocking with sonicated salmon sperm DNA (Stratagene, La Jolla, CA) and hybridized at 42°C overnight with the labeled probe rotating. Washings were carried out in 2× SSC, 0.1% SDS, for 10 min at room temperature, 1× SSC, 0.1% SDS, for 1 hr at 42°C, and 0.2× SSC, 0.1% SDS, at 42°C for 1 hr. A BAS imaging plate (Fuji Photo Film Co. Ltd., Kanagawa, Japan) was exposed to the filter for 2 hr, and relative band intensities were measured with a BAS 2000 system (Fuji).

Growth-inhibition assay

The effect of hnRNP L on cell sensitivity to KW2189 was estimated by the 3-(4,5-dimethylthiazol-2yl)-2,5-diphenoyltetrazoliumbromide (MTT) assay. NIH3T3, and stable transfectants of hnRNP L cDNA, Fw3and Fw9 cells were exposed to 0–50 nM KW2189 for 72 hr before measuring absorbance. The OD values at 562–630 nm were measured with a 96-well microtiter plate reader, EL340 (Bio-Tek, Winooski, VT).

Immunochemical cell staining

Human lung cancer cell lines, SBC-3, PC-9, PC-14 and H69 cells were prepared on slide glasses with cytospin (Shandon, Pittsburgh, PA). The cells were dried and then fixed in cold acetone for 2 min. All of the incubation steps were carried out at room temperature, and Step 2 and 3 were carried out in the dark. The steps included: 1) incubation with 10% horse serum for 30 min for blocking; 2) incubation with anti-human hnRNP L (1:500 diluted in PBS with 1.5% blocking serum) for 60 min; and 3) incubation with fluorescence anti-mouse IgG (1:500 diluted) for 45 min. Slides were washed with 3 changes of PBS between each step. After Step 2 each washing was carried out for 5 min. The slides were mounted with 90% glycerol in PBS and examined with a fluorescence microscope (Nikon, Tokyo, Japan), equipped with fluorescein isothiocyanate filter set B-2A (Nikon).

EGFP-hnRNP L deletion mutants

pRc/CMV containing the 14–1718 fragment of hnRNP L cDNA (2033bp) was constructed as described above. After digesting the plasmid with SacII and BamHI, and the resulting fragment was introduced into the SacII/BamHI site of the pEGFP-C3 vector (Clontech, Palo Alto, CA), with the Takara DNA ligation system. Construction of deletion plasmids was carried out as follows. EGFP-hnRNP L (Construct 2) was partially digested with StuI and self-ligated to generate Constructs 3 and 6. PEGFP-hnRNP L was digested with BglII, and after extracting the 570 bp and 1023 bp fragments with a QIAquick Gel Extraction Kit (Qiagen, Hilden, Germany), each fragment was inserted into the BglII site of the pEGFP-C2 and -C3 vectors to generate Constructs 4 and 7, respectively. The 384 bp fragment of hnRNP L extracted by digesting with StuI was inserted into the SmaI site of pEGFP-C3 vectors to generate Construct 5. PEGFP-hnRNP L was digested with KpnI, and it self-ligated to generate Construct 8. The 584 bp fragment digested with KpnI and BglII and extracted was inserted into the BglII site of pEGFP-C3 vectors to generate Construct 9, and the 626 bp fragment digested with AccI was inserted into the AccI site of pEGFP-C3 vectors to generate Construct 10 (Fig. 1).

A cover-glass was placed on the bottom of each well of a 6-well culture dish, and each well was seeded with 1.6×10^5 NIH3T3 cells and incubated for 48 hr at 37°C. After diluting 2.5 μg/well of plasmid

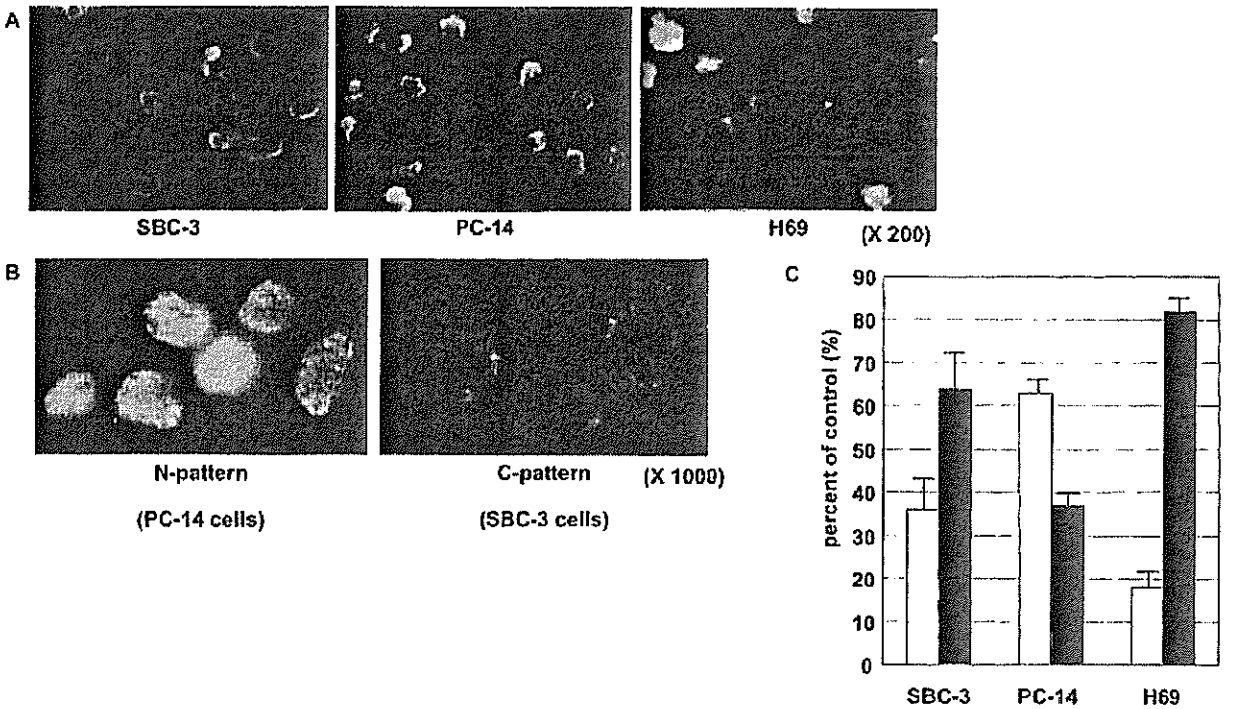

FIGURE 6 – Immunochemical staining of hnRNP L in human lung cancer cells. (*a*) Immunochemical cell staining was carried out using anti-hnRNP L antibody as the primary antibody and fluorescent anti-mouse IgG as the secondary antibody. (*b*) Intracellular localization of hnRNP L. (*c*) Cells were classified into N (white column) or C (gray column) patterns. Three independent cell counts were carried out.

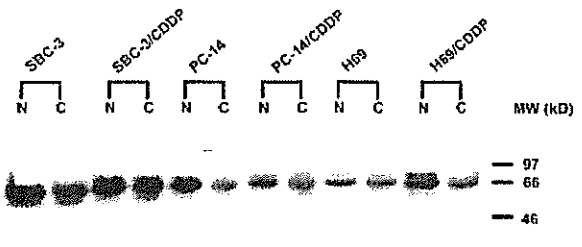

FIGURE 7 – Intracellular expression of hnRNP L in human lung cancer cell lines. The nuclear (N) and cytoplasmic (C) fractions of the cells were isolated as described in Material and Methods. Western blot analysis was carried out using anti-hnRNP L antibody. The cisplatin-resistant sublines were also examined to determine whether the localization patterns depended on the cell type.

DNA (pEGFP vectors containing deletion mutants of hnRNP L described above) in 1 ml/well of serum-free DMEM, 7.5 μl/well of 1 mM TransFast Reagent (Promega, Madison, WI) was added to the mixture. After allowing the mixture to stand for 15 min at room temperature, it was added to cells from which the growth medium was removed. The cells were then incubated for 1 hr at 37°C, and 1 ml/well of complete growth medium was added to them. At 24 hr after transfection, the cells were mounted on slides with aqueous mounting medium and examined under a fluorescence microscope (Nikon, B-2A filter, Tokyo, Japan).

RESULTS

Purification and sequence analysis of the DARP

Purification of the DARP was conducted as described previously.[9] After affinity purification, 2 main proteins were detected in SDS-PAGE with silver staining. Further purification efforts with DEAE-sephacel column chromatography gave a single band of Mr ~60,000 with the binding activity to the labeled duocarmycin-modified oligonucleotides (Fig. 2*a*). Coincubation of duocarmycin-treated calf thymus DNA with the labeled probe and purified DARP resulted in the retarded band in the gel mobility shift assay (Fig. 2*b*). Competition experiment in the presence of 30 and 300 ng of calf thymus DNA-DUMSA adduct demonstrated that 300 ng adduct reduced the intensity of the band in our previous study.[9]

The 60 kDa protein separated by SDS-PAGE was excised and digested with lysyl endopeptidase. The resulting peptides were eluted, separated by reversed phase HPLC, and sequenced. Three partial amino acid sequences were obtained, AAAGGGGGGGRYYGGG, DFSESRNNRFSTPEQAA and SDALETLGFLN, which were found to completely match parts of the predicted human heterogeneous nuclear ribonucleoprotein L. Gel mobility shift assay using anti-hnRNP L did not, however, show the supershift of the band induced by anti-hnRNP L (data not shown).

Expression of hnRNP L

Western blot analysis was carried out using a membrane containing normal human tissue lysates from different organs. A 68 kDa band of hnRNP L was detected in total protein extracts from brain and small intestine, but not in others, including normal lung (Fig. 3). The expression of hnRNP L protein, however, was detected in the human lung cancer cell lines (Fig. 4*a*). Northern blot analysis confirmed the expression of hnRNP L at the mRNA (~2 kbp) level in these cells (Fig. 4*b*). In contradiction to our first result that hnRNP L was not detected in normal lung tissue, the expression of hnRNP L in malignant cells seemed to increase.

Effect of hnRNP L on drug sensitivity

To evaluate the function of hnRNP L, hnRNP L cDNA was transfected into NIH3T3 cells, and stable transfectant clones were

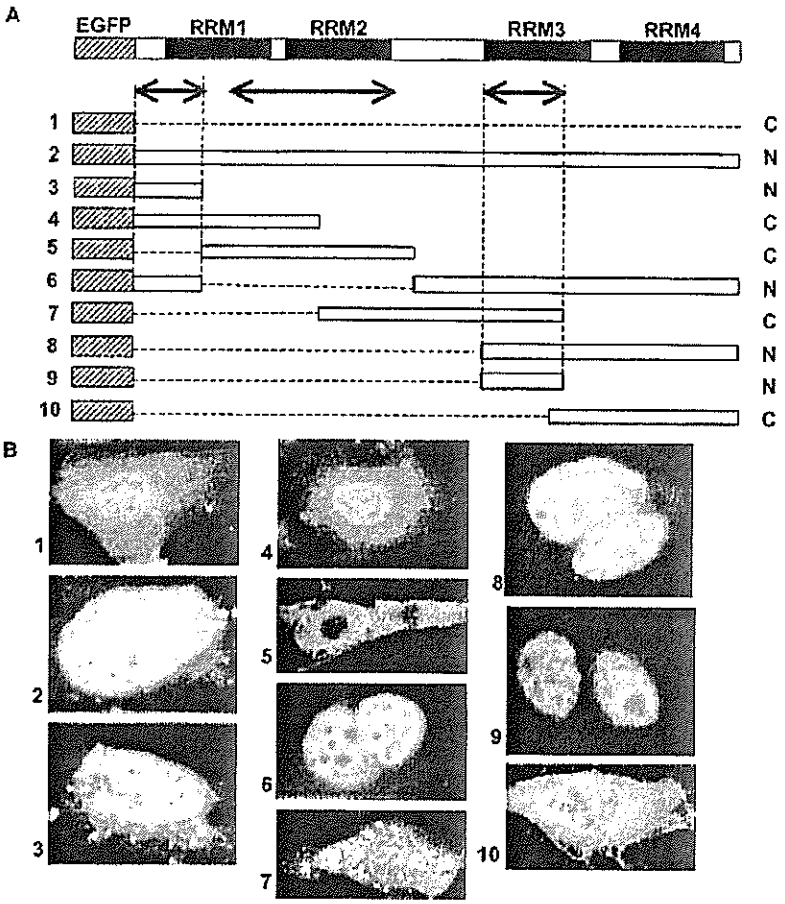

FIGURE 8 – Effect of hnRNP L deletion on the intracellular localization of EGFP-hnRNP L. (*a*) Arrows indicate the part expected to be responsible for localization of hnRNP L. Letters N (nuclear localization) and C (cytoplasmic localization) at the right end indicate the results of classification by the transfection study. (*b*) Localization of EGFP-hnRNP L deletion mutants. NIH3T3 cells were transfected with each construct, and they were examined by fluorescent microscopy to identify the localization of EGFP-fusion. The numbers correspond to those of the constructs in (*a*).

characterized. The Fw3 and Fw9 clones showed higher expression of hnRNP L mRNA than other transfectants by 5.2-fold and 4.4-fold to control respectively detected by Northern blot analysis (Fig. 5*a*).

We measured the growth inhibitory effect of KW-2189 in the hnRNP L transfectant cells by MTT assay. The IC_{50} values for KW-2189 in the Fw3 and Fw9 clones were 3.5 nM and 4.3 nM, respectively, and the Fw3 and Fw9 cells were 13.4-fold and 10.9-fold, respectively, more sensitive to KW-2189 than the Mock transfectant C4 cells (IC_{50}: 47 nM) (Fig. 5*b*). These results indicate that hnRNP L enhances cell sensitivity to the growth inhibitory effect of KW-2189 *in vitro*. We also examined the sensitivity of the transfectants to cisplatin and mitomycin C and no difference of the sensitivity was observed between the transfectants and the Mock cells (data not shown). The hnRNPs have been reported to regulate both nuclear and cytoplasmic events, as described above, and the intracellular localization of hnRNP L was examined in the next step to identify the site of action of hnRNP L in the sensitivity enhancement machinery.

Localization of hnRNP L protein in human lung cancer cell lines

We carried out immunofluorescence cell staining with anti-hnRNP L antibody to determine the subcellular localization of hnRNP L protein in human lung cancer cells (Fig. 6*a*). Based on the results, the localization of hnRNP L cells could be classified into two patterns: nuclear localization (N) and cytoplasmic localization (C) (Fig. 6*b*). As shown in Figure 6*c*, the cytoplasmic pattern was observed frequently in SBC-3 and H69 cells, whereas the nuclear pattern was common in PC-14 cells. To confirm this differential distribution, fractionated proteins from the nuclear and cytoplasmic fractions of these cells were immunoblotted with anti-hnRNP L antibody (Fig. 7). The results showed that hnRNP L was expressed equally in the nucleus and cytoplasm of the SBC-3 and H69 cells, whereas it was expressed predominantly in the nuclei of the PC-14 cells. These results are consistent with the immunocytological findings. In addition, the cisplatin-resistant sublines derived from these cells exhibited the same localization pattern as their parental cells. This indicates that the differential localization depends on the cell type.

Motifs required for the intracellular localization of hnRNP L

It has been reported that hnRNP L is localized in the nucleoplasm of HeLa cells, except the nucleoli,[12] but the mechanism of its localization remains unknown. To identify the motifs responsible for the localization of hnRNP L, we constructed an hnRNP L deletion series fused to EGFP (Fig. 8*a*), transfected the constructs into NIH3T3 cells, and examined them under a fluorescence microscope. As shown in Figure 8*b*, EGFP protein itself was rather evenly distributed throughout the cell, the cytoplasm and the nucleus (Transfectant 1). Full-length hnRNP L was present in the nucleoplasm, except the nucleoli (Transfectant 2). Deletion mutants containing the N-terminal portion of RRM1 or of RRM3 (Transfectants 3, 6, 8 and 9) showed hnRNP L localization in the nucleus. Transfectants 4, 5 and 7, containing the N-terminal portion of RRM2 showed hnRNP L distributed through the cell, whether they also contained that portion of RRM1 and RRM3 or not. In Transfectant 10, which lacked the N-terminal region of all

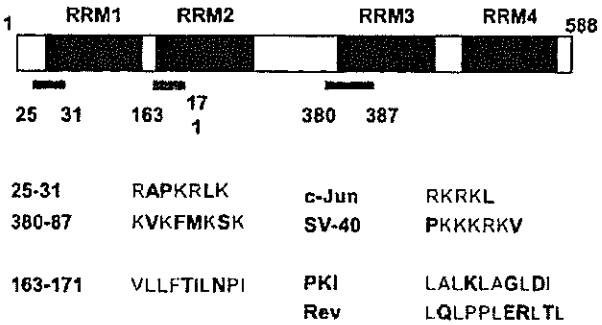

FIGURE 9 – NLS-like and NES-like sequences in hnRNP L. There are 2 NLS-like sequences that resemble the NLS sequences of c-Jun and SV-40 large T antigen and one NES-like sequence that resembles the NES sequences of PKI and Rev.

3 RRMs, hnRNP L was distributed throughout the cell. These results indicate that the N-terminal portion of each RRM is required for determination of the intracellular localization of hnRNP L (Fig. 8*a*, *arrows*). We then searched the sequence of hnRNP L and found 2 sequences that were rich in alkaline amino acids (residues 25–31, 380–387) and a sequence that was rich in hydrophobic amino acids (residue 163–171, Fig. 9). The sequences rich in alkaline amino acids showed high homology with the NLS sequences of c-Jun and SV40 large T antigen,[13,14] and the sequence rich in hydrophobic amino acids showed high homology with the NES sequences of PKI[15] and Rev[16] respectively. The N-terminal portion of RRM1 and RRM3 contain the NLS-like sequences, residue 25–31 and residue 380–387, respectively, and the N-terminal portion of RRM2 contains the NES-like sequence, residue 163–171.

DISCUSSION

There are approximately 20 major hnRNPs, and some of them have been reported to be highly expressed in cancer tissues. Sueoka *et al.*[3] demonstrated elevated expression of hnRNP B1 mRNA in human lung cancer tissue, and hnRNP I and hnRNP K mRNA have been reported in malignant glioblastoma and breast cancer, respectively.[2,17] We demonstrated expression of hnRNP L in human lung cancer cell lines and high expression of hnRNP L is presumably present in lung cancer tissue.

We reported previously that a nuclear protein in human cancer cells binds to the DUM-DNA adduct. The protein, DARP, preferentially bound to the DNA damage induced by DNA-alkylating minor groove binders such as DUMs and CC-1065. Because the amino acid sequence of DARP was identical to hnRNP L, hnRNP L is a candidate protein that binds to the DNA damage induced by DUM. A water-soluble derivative of DUM, KW-2189, exhibits broad spectrum antitumor activity in a series of experimental tumor models and entered clinical trials. KW-2189 was designed as a prodrug to generate active species, DU86, in tumor cells and DARP bounds to the DNA induced by DU86 (unpublished results). Although KW-2189 alkylates DNA *in vitro*, only the DU86-DNA adduct was detected in the human cells treated with KW-2189.[18,19] The transfection study demonstrated that hnRNP L enhanced the cellular sensitivity to KW2189. As described previously, DARP did not recognize the DNA adducts of cisplatin and mitomycin C *in vitro*.[18] We show that when we examined the transfectants for sensitivity to other DNA-damaging agents, *i.e.*, the major groove binders mitomycin C and cisplatin (data not shown), ectopic hnRNP L expression had no affect on cell sensitivity to them. These results suggest that DARP could be hnRNP L and it acts specifically on DNA damage induced by the minor groove binder.

Other possible mechanisms of increased sensitivity to KW-2189 are: 1) that hnRNP L facilitates transportation of the drug to the nucleus, and 2) that hnRNP L increases the stability of the drug-DNA adduct in a sequence-specific manner.

We have described the difference in intracellular localization of hnRNP L in human lung cancer cell lines. Although there is a report claiming that hnRNP L localized in the nucleoplasm in HeLa cells transfected with hnRNP L,[12] we showed that the intracellular localization of hnRNP L differs among human lung cancer cell lines.

There was a report that hnRNP A2 is located in the cytoplasm in post-mitotic phase.[20] In this study, few mitotic cells were observed in the culture condition indicating that mitosis was not correlated with hnRNP L distribution. We speculate that in the case of hnRNP A2 a different mechanism might be involved in the intracellular localization of hnRNP L. Nevertheless, synchronization experiments must be examined.

SBC-3 and PC-14 cells grow faster than H69 cells. Even though cell growths of SBC-3 and PC-14 cells were equal in our culture condition, distribution of hnRNP L in these cells were different. This result indicate that the distribution depends on the cell type rather than difference of the cell growth.

To determine whether the localization of hnRNP L is altered by drug exposure, we examined the immunofluorescent staining of hnRNP L in lung cancer cells exposed to KW-2189 for 24 hr. An increased population of cells in which hnRNP L was localized in the nucleus was observed after exposure of a small cell lung cancer (SBC-3) cell line to KW-2189 (data not shown). Although this result was not observed in the rest two cell lines, it can support the hypothesis that hnRNP L helps drugs to transport into nuclear and involves in cell sensitivity mentioned above.

To test the hypothesis that the differences in intracellular localization in lung cancer cells are due to gene alterations, we compared the hnRNP L cDNA sequences in these cell lines. No mutations were detected in any of the lines (data not shown), suggesting that hnRNP L might be co-localized with other proteins. Interaction between hnRNPs has been reported and hnRNP L is known to have a binding domain for interaction with other hnRNPs (*e.g.*, hnRNP I and hnRNP K),[21] which are recognized to have NLS. Based on this evidence, the differences in localization of hnRNP L in these cell lines might be due to changes in the molecules that interact with hnRNP L, such as hnRNP I or K. In addition, the putative sites for regulation of localization signal in hnRNP L that we found (25–31, 380–387 and 163–171) would be involved in these interactions. Further studies should extend the potential use of hnRNP L as a factor to assess sensitivity to chemotherapy and candidate molecules for drug development. In addition, expression of hnRNP L needs to be investigated in tissue from lung cancer patients for therapeutic exploitation.

In summary, we have demonstrated the expression of hnRNP L with different intracellular localization in human lung cancer cell lines and that ectopic hnRNP L expression increases cellular sensitivity to a minor groove binder.

ACKNOWLEDGEMENT

The authors are grateful to Dr. G. Dreyfuss for providing anti-hnRNP L antibody.

REFERENCES

1. Dreyfuss G, Matunis MJ, Pinol-Roma S, Burd CG. hnRNP proteins and the biogenesis of mRNA. Annu Rev Biochem 1993;62:289–321.
2. Jin W, McCutcheon IE, Fuller GN, Huang ES, Cote GJ. Fibroblast growth factor receptor-1 α-exon exclusion and polypyrimidine tract-binding protein in glioblastoma multiforme tumors. Cancer Res 2000; 60:1221–4.

3. Sueoka E, Goto Y, Sueoka N, Kai Y, Kozu T, Fujiki H. Heterogeneous nuclear ribonucleoprotein B1 as a new marker of early detection for human lung cancers. Cancer Res 1999;59:1404–7.
4. Shih SC, Claffey KP. Regulation of human vascular endothelial growth factor mRNA stability in hypoxia by heterogeneous nuclear ribonucleoprotein L. J Biol Chem 1999;274:1359–65.
5. Liu X, Mertz JE. HnRNP L binds a *cis*-acting RNA sequence element that enables intron-dependent gene expression. Genes Dev 1995;9: 1766–80.
6. Ogasawara H, Nishio K, Takeda Y, Ohmori T, Kubota N, Funayama Y, Ohira T, Kuraishi Y, Isogai Y, Saijo N. A novel antitumor antibiotic, KW-2189 is activated by carboxyl esterase and induces DNA strand breaks in human small cell lung cancer cells. Jpn J Cancer Res 1994;85:418–25.
7. Ogasawara H, Nishio K, Kanzawa F, Lee YS, Funayama Y, Ohira T, Kuraishi Y, Isogai Y, Saijo N. Intracellular carboxyl esterase activity is a determinant of cellular sensitivity to the antineoplastic agent KW-2189 in cell lines resistant to cisplatin and CPT-11. Jpn J Cancer Res 1995;86:124–9.
8. Ogasawara H, Nishio K, Ishida T, Arioka H, Fukuoka K, Saijo N. *In vitro* enhancement of antitumor activity of a water-soluble duocarmycin derivative, KW-2189, by caffeine-mediated DNA-repair inhibition in human lung cancer cells. Jpn J Cancer Res 1997;88:1033–7.
9. Asai A, Yano K, Mizukami T, Nakano H. Characterization of a duocarmycin-DNA adduct-recognizing protein in cancer cells. Cancer Res 1999;59:5417–20.
10. Kasahara K, Fujiwara Y, Nishio K, Ohmori T, Sugimoto Y, Komiya K, Matsuda T, Saijo N. Metallothionein content correlates with the sensitivity of human small cell lung cancer cell lines to cisplatin. Cancer Res 1991;51:3237–42.
11. Ohmori T, Morikage T, Sugimoto Y, Fujiwara Y, Kasahara K, Nishio K, Ohta S, Sasaki Y, Takahashi T, Saijo N. The mechanism of the difference in cellular uptake of platinum derivatives in non-small cell lung cancer cell line (PC-14) and its cisplatin-resistant subline (PC-14/CDDP). Jpn J Cancer Res 1993;84:83–92.
12. Hahm B, Cho OH, Kim JE, Kim YK, Kim JH, Oh YL, Jang SK. Polypyrimidine tract-binding protein interacts with HnRNP L. FEBS Lett 1998;425:401–6.
13. Kalderon D, Richardson WD, Markham AF, Smith AE. Sequence requirements for nuclear location of simian virus 40 large-T antigen. Nature 1984;311:33–8.
14. Lanford RE, Butel JS. Construction and characterization of an SV40 mutant defective in nuclear transport of T antigen. Cell 1984;37:801–13.
15. Wen W, Meinkoth JL, Tsien RY, Taylor SS. Identification of a signal for rapid export of proteins from the nucleus. Cell 1995;82:463–73.
16. Fischer U, Huber J, Boelens WC, Mattaj IW, Luhrmann R. The HIV-1 Rev activation domain is a nuclear export signal that accesses an export pathway used by specific cellular RNAs. Cell 1995;82:475–83.
17. Mandal M, Vadlamudi R, Nguyen D, Wang RA, Costa L, Bagheri-Yarmand R, Mendelsohn J, Kumar R. Growth factors regulate heterogeneous nuclear ribonucleoprotein K expression and function. J Biol Chem 2001;276:9699–704.
18. Asai A, Nagamura S, Saito H, Takahashi I, Nakano H. The reversible DNA-alkylating activity of duocarmycin and its analogues. Nucleic Acids Res 1994;22:88–93.
19. Okamoto A, Asai A, Saito H, Okabe M, Gomi K. Differential effect of duocarmycin A and its novel derivative DU-86 on DNA strand breaks in HeLa S3 cells. Jpn J Cancer Res 1994;85:1304–11.
20. Kim JH, Hahm B, Kim YK, Choi M, Jang SK. Protein-protein interaction among hnRNPs shuttling between nucleus and cytoplasm. J Mol Biol 2000;298:395–405.
21. Kamma H, Satoh H, Matusi M, Wu WW, Fujiwara M, Horiguchi H. Characterization of hnRNP A2 and B1 using monoclonal antibodies: intracellular distribution and metabolism through cell cycle. Immunol Lett 2001;76:49–54.

Differential Constitutive Activation of the Epidermal Growth Factor Receptor in Non–Small Cell Lung Cancer Cells Bearing *EGFR* Gene Mutation and Amplification

Takafumi Okabe,[1] Isamu Okamoto,[1] Kenji Tamura,[3] Masaaki Terashima,[1] Takeshi Yoshida,[1] Taroh Satoh,[1] Minoru Takada,[2] Masahiro Fukuoka,[1] and Kazuhiko Nakagawa[1]

[1]Department of Medical Oncology, Kinki University School of Medicine; [2]National Kinki Central Chest Medical Center, Osaka, Japan; and [3]Department of Medical Oncology, Nara Hospital, Kinki University School of Medicine, Nara, Japan

Abstract

The identification of somatic mutations in the tyrosine kinase domain of the epidermal growth factor receptor (EGFR) in patients with non–small cell lung cancer (NSCLC) and the association of such mutations with the clinical response to EGFR tyrosine kinase inhibitors (TKI), such as gefitinib and erlotinib, have had a substantial effect on the treatment of this disease. *EGFR* gene amplification has also been associated with an increased therapeutic response to EGFR-TKIs. The effects of these two types of *EGFR* alteration on EGFR function have remained unclear, however. We have now examined 16 NSCLC cell lines, including eight newly established lines from Japanese NSCLC patients, for the presence of *EGFR* mutations and amplification. Four of the six cell lines that harbor *EGFR* mutations were found to be positive for *EGFR* amplification, whereas none of the 10 cell lines negative for *EGFR* mutation manifested *EGFR* amplification, suggesting that these two types of *EGFR* alteration are closely associated. Endogenous EGFRs expressed in NSCLC cell lines positive for both *EGFR* mutation and amplification were found to be constitutively activated as a result of ligand-independent dimerization. Furthermore, the patterns of both *EGFR* amplification and EGFR autophosphorylation were shown to differ between cell lines harboring the two most common types of *EGFR* mutation (exon 19 deletion and L858R point mutation in exon 21). These results reveal distinct biochemical properties of endogenous mutant forms of EGFR expressed in NSCLC cell lines and may have implications for treatment of this condition. [Cancer Res 2007;67(5):2046–53]

Introduction

The epidermal growth factor receptor (EGFR) is a 170-kDa transmembrane glycoprotein with an extracellular ligand binding domain, a transmembrane region, and a cytoplasmic tyrosine kinase domain and is encoded by a gene (*EGFR*) located at human chromosomal region 7p12 (1–3). The binding of ligand to EGFR induces receptor dimerization and consequent conformational changes that result in activation of the intrinsic tyrosine kinase, receptor autophosphorylation, and activation of a signaling cascade (4, 5). Aberrant signaling by EGFR plays an important role in cancer development and progression (3).

EGFR is frequently overexpressed in non–small cell lung cancer (NSCLC) and has been implicated in the pathogenesis of this disease (6, 7). Given the biological importance of EGFR signaling in cancer, several agents have been synthesized that inhibit the receptor tyrosine kinase activity. Two such inhibitors of the tyrosine kinase activity of EGFR (EGFR-TKI), gefitinib and erlotinib, both of which compete with ATP for binding to the tyrosine kinase pocket of the receptor, have been extensively studied in patients with NSCLC (8, 9). We and others have shown that a clinical response to these agents is more common in women than in men, in Japanese than in individuals from Europe or the United States, in patients with adenocarcinoma than in those with other histologic subtypes of cancer, and in patients who have never smoked than in those with a history of smoking (10–14). Mutations in the tyrosine kinase domain of EGFR have also been detected in a subset of lung cancer patients and shown to predict sensitivity to EGFR-TKIs (15–17). Indeed, the clinical characteristics of patients with known *EGFR* mutations are similar to those of other individuals most likely to respond to treatment with EGFR-TKIs (18–22). These mutations arise in the first four exons (exons 18–21) corresponding to the tyrosine kinase domain of EGFR, and they affect key amino acids surrounding the ATP-binding cleft (23, 24). In-frame deletions that eliminate four highly conserved amino acids (LREA) encoded by exon 19 are the most common type of *EGFR* mutation, with missense point mutations in exon 21 that result in a specific amino acid substitution at position 858 (L858R) being the second most common. In addition to *EGFR* mutations, other molecular changes may play a role in determining sensitivity to EGFR-TKIs (22, 25–28). NSCLC patients with an increased *EGFR* copy number, as revealed by fluorescence *in situ* hybridization (FISH), have thus been found to show an increased response rate to and prolonged survival after gefitinib therapy (22, 25–27).

Given that *EGFR* is mutated or amplified (or both) in NSCLC, it is important to determine the biological effects of such *EGFR* alterations on EGFR function (15, 29–32). Transient transfection of various cell types with vectors encoding wild-type or mutant versions of EGFR showed that the activation of mutant receptors by EGF is more pronounced and sustained than is that of the wild-type receptor (15, 30). However, detailed biochemical analysis of NSCLC cell lines with endogenous *EGFR* mutations has been limited. We have now identified *EGFR* mutations in three NSCLC cell lines newly established from Japanese patients. Furthermore, we have characterized a panel of 16 NSCLC cell lines for *EGFR* mutations and amplification and evaluated the relation between the presence of these two types of *EGFR* alteration and sensitivity to gefitinib. The effects of *EGFR* alterations on activation status of EGFR and on downstream signaling were also evaluated.

Requests for reprints: Isamu Okamoto, Department of Medical Oncology, Kinki University School of Medicine, 377-2, Ohno-higashi, Osaka-Sayama, Osaka 589-8511, Japan. Phone: 81-72-366-0221; Fax: 81-72-360-5000; E-mail: okamoto@dotd.med.kindai.ac.jp.

doi:10.1158/0008-5472.CAN-06-3339

Finally, in *EGFR* mutant cell lines showing constitutive EGFR activation, we assessed how the mutations activate the tyrosine kinase domain of the receptor.

Materials and Methods

Cell lines. The human NSCLC cell lines NCI-H226 (H226), NCI-H292 (H292), NCI-H460 (H460), NCI-H1299 (H1299), NCI-H1650 (H1650), and NCI-H1975 (H1975) were obtained from the American Type Culture Collection (Manassas, VA). PC-9 and A549 cells were obtained as described previously (33). Ma-1 cells were kindly provided by E. Shimizu (Tottori University, Yonago, Japan). We established seven cell lines (KT-2, KT-4, Ma-25, Ma-31, Ma-34, Ma-45, and Ma-53) from tissue or pleural effusion of Japanese patients with advanced NSCLC. These cell lines were cultured under a humidified atmosphere of 5% CO_2 at 37°C in RPMI 1640 (Sigma, St. Louis, MO) supplemented with 10% fetal bovine serum. Informed consent for establishment of cell lines and tumor DNA sequencing was obtained in accordance with the ethical guidelines for human genome/genetic analysis in Japan.

Growth inhibition assay. Gefitinib was kindly provided by AstraZeneca (Macclesfield, United Kingdom) as a pure substance and was diluted in DMSO to obtain a stock solution of 20 mmol/L. For growth inhibition assays, cells (0.5×10^4 to 4.5×10^4) were plated in 96-well flat-bottomed plates and cultured for 24 h before the addition of various concentrations of gefitinib and incubation for an additional 72 h. TetraColor One (5 mmol/L tetrazolium monosodium salt and 0.2 mmol/L 1-methoxy-5-methyl phenazinium methylsulfate; Seikagaku, Tokyo, Japan) was then added to each well, and the cells were incubated for 3 h at 37°C before measurement of absorbance at 490 nm with a Multiskan Spectrum instrument (Thermo Labsystems, Boston, MA). Absorbance values were expressed as a percentage of that for untreated cells, and the concentration of gefitinib resulting in 50% growth inhibition (IC_{50}) was calculated.

Genetic analysis of *EGFR*. Genomic DNA was extracted from cell lines with the use of a QIAamp DNA Mini kit (Qiagen, Tokyo, Japan), and exons 18 to 21 of *EGFR* were amplified by the PCR and sequenced directly. PCR was done in a reaction mixture (25 μL) containing 50 ng of genomic DNA and TaKaRa Taq polymerase (TaKaRa BIO, Tokyo, Japan) and with an initial incubation for 3 min at 94°C followed by 30 cycles of 20 s at 94°C, 30 s at 58°C, and 20 s at 72°C and by a final incubation for 7 min at 72°C. The PCR products were purified with a Microcon YM-100 filtration device (Millipore, Billerica, MA) before sequencing with the use of an ABI BigDye Terminator v. 3.1 Cycle Sequencing kit (Applied Biosystems, Foster City, CA). Sequencing reaction mixtures were subjected to electrophoresis with an ABI PRISM 3100 Genetic Analyzer (Applied Biosystems). Primers for mutation analysis (sense and antisense, respectively) were as follows: exon 18, 5′-CAAATGAGCTGGCAAGTGCCGTGTC-3′ and 5′-GAGTTTCCCAAACACTCAGTGAAA-C-3′; exon 19, 5′-GCAATATCAGCCTTAGGTGCGGCTC-3′and 5′-CATAGAAAGTGAACATTTAGGATGTG-3′; exon 20, 5′-CCATGAGTACGTATTTTGAAACTC-3′ and 5′-CATATCCCCATGGCAAACTCTTGC-3′; and exon 21, 5′-CTAACGTTCGCCAGCCATAAGTCC-3′ and 5′-GCTGCGAGCTCACCCAGAATGTCTGG-3′.

FISH. *EGFR* copy number per cell was determined by FISH with the use of the LSI EGFR Spectrum Orange and CEP7 Spectrum Green probes (Vysis; Abbott, Des Plaines, IL). Cells were centrifuged onto glass slides with a Shandon cytocentrifuge (Thermo Electron, Pittsburgh, PA) and fixed by consecutive incubations with ice-cold 70% ethanol for 10 min, 85% ethanol for 5 min, and 100% ethanol for 5 min. Slides were stored at −20°C until analysis. Cells were subsequently subjected to digestion with pepsin for 10 min at 37°C, washed with water, dehydrated with a graded series of ethanol solutions, denatured with 70% formamide in 2× SSC for 5 min at 72°C, and dehydrated again with a graded series of ethanol solutions before incubation with a hybridization mixture consisting of 50% formamide, 2× SSC, Cot-1 DNA, and labeled DNA. The slides were washed for 5 min at 73°C with 3× SSC, for 5 min at 37°C with 4× SSC containing 0.1% Triton X-100, and for 5 min at room temperature with 2× SSC before counterstaining with antifade solution containing 4′,6-diamidino-2-phenylindole. Hybridization signals were scored in 40 nuclei with the use of a ×100 immersion objective. Nuclei with a disrupted boundary were excluded from the analysis. Gene amplification was defined by an *EGFR*/chromosome 7 copy number ratio of ≥2 or by the presence of clusters of ≥15 copies of *EGFR* per cell in ≥10% of cells, as described previously (25, 27).

Immunoblot analysis. Cell lysates were fractionated by SDS-PAGE on a 7.5% gel, and the separated proteins were transferred to a nitrocellulose membrane. After blocking of nonspecific sites with 5% skim milk, the membrane was incubated overnight at room temperature with primary antibodies. Antibodies to phosphorylated EGFR (pY845, pY1068, or pY1173), extracellular signal-regulated kinase (ERK), phosphorylated AKT, AKT, Src homology and collagen (Shc), and phosphorylated Shc were obtained from Cell Signaling Technology (Beverly, MA); antibodies to EGFR were from Zymed (South San Francisco, CA); antibodies to phosphorylated ERK were from Santa Cruz Biotechnology (Santa Cruz, CA); and antibodies to β-actin (loading control) were from Sigma. Immune complexes were detected by incubation of the membrane for 1 h at room temperature with horseradish peroxidase–conjugated goat antibodies to mouse or rabbit immunoglobulin (Amersham Biosciences, Little Chalfont, United Kingdom) and by subsequent exposure to enhanced chemiluminescence reagents (Perkin-Elmer, Boston, MA).

Table 1. Characteristics of NSCLC cell lines

Cell lines	Gefitinib IC_{50} (μmol/L)	*EGFR* mutation	*EGFR* amplification	Histology
PC-9	0.07	del(E746-A750)	+	Adenocarcinoma
KT-2	0.57	L858R	+	Adenocarcinoma
KT-4	1.26	L858R	+	Large cell carcinoma
Ma-1	2.34	del(E746-A750)	+	Adenocarcinoma
H1650	6.66	del (E746-A750)	–	Adenocarcinoma
A549	8.70	Wild type	–	Adenocarcinoma
H1975	9.32	L858R+T790M	–	Adenocarcinoma
H292	9.44	Wild type	–	Mucoepidermoid carcinoma
H226	9.53	Wild type	–	Squamous cell carcinoma
Ma-25	10.17	Wild type	–	Large cell carcinoma
H460	10.38	Wild type	–	Large cell carcinoma
Ma-45	10.47	Wild type	–	Adenocarcinoma
Ma-53	10.47	Wild type	–	Adenocarcinoma
Ma-34	11.17	Wild type	–	Adenocarcinoma
H1299	11.28	Wild type	–	Large cell carcinoma
Ma-31	12.46	Wild type	–	Adenocarcinoma

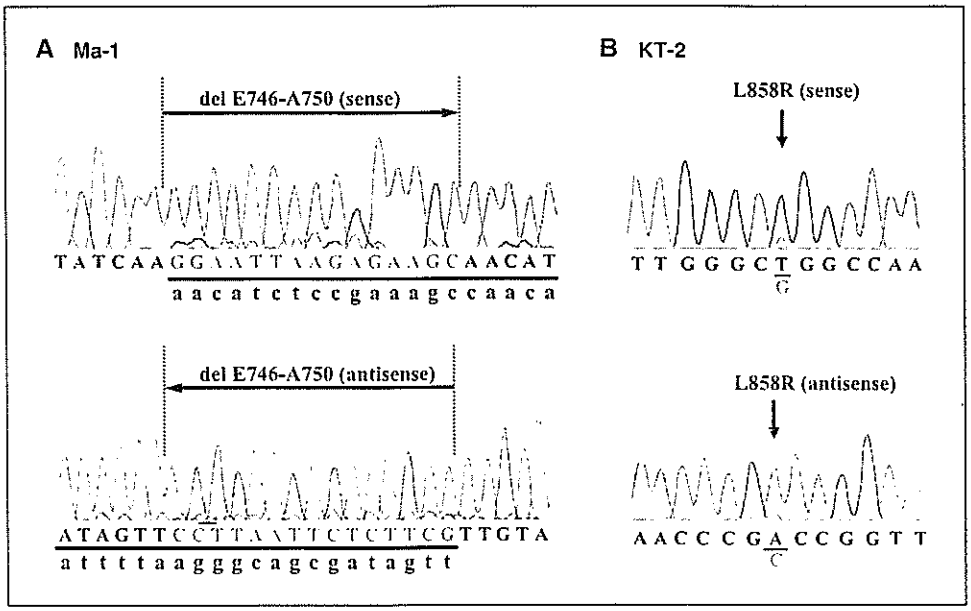

Figure 1. Detection of *EGFR* mutations in NSCLC cell lines. The portions of the sequencing electrophoretograms corresponding to the mutations are shown for Ma-1 (*A*) and KT-2 (*B*) cells. *A*, heterozygous in-frame deletion in exon 19 is revealed by the presence of double peaks. Tracings in both sense and antisense directions are shown to highlight the two breakpoints of the deletion. Wild-type (*uppercase*) and mutant (*lowercase*) nucleotide sequences. *B*, heterozygous point mutation (T — G) at nucleotide position 2819 in exon 21.

Treatment of cells with neutralizing antibodies. Cells were exposed to neutralizing antibodies (each at 12 μg/mL) for 3 h before EGF stimulation. The antibodies included those to EGF and to transforming growth factor-α (TGF-α), both from R&D Systems (Minneapolis, MN) as well as antibodies to EGFR (Upstate Biotechnology, Lake Placid, NY). Cell lysates were then prepared and subjected to immunoblot analysis with antibodies to phosphorylated EGFR (pY1068) and to EGFR as described above.

Chemical cross-linking assay. Chemical cross-linking was done as described previously (34, 35). Cells were washed twice with ice-cold PBS and then incubated for 20 min at 4°C with 1 mmol/L bis(sulfosuccinimidyl)-suberate (Pierce, Rockford, IL) in PBS. The cross-linking reaction was terminated by the addition of glycine to a final concentration of 250 mmol/L and incubation for an additional 5 min at 4°C. The cells were washed with PBS, and cell lysates were resolved by SDS-PAGE on a 4% gel and subjected to immunoblot analysis with anti-EGFR (Santa Cruz Biotechnology).

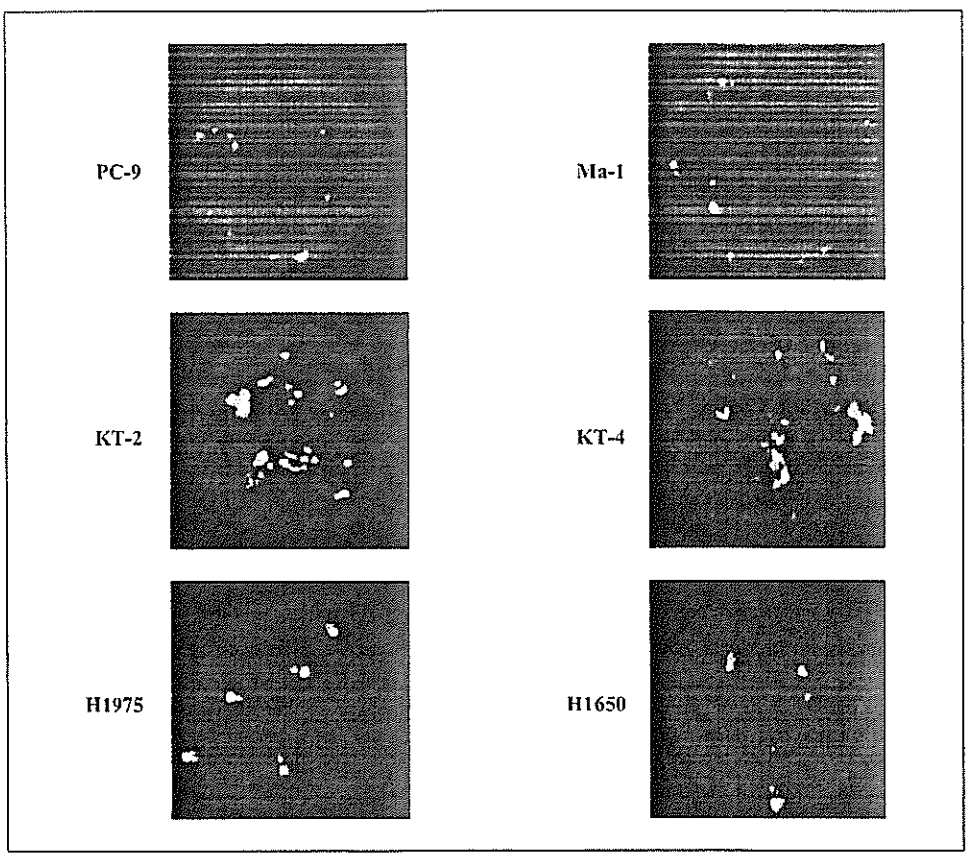

Figure 2. FISH analysis of *EGFR* amplification in NSCLC cell lines. The analysis was done with probes specific for *EGFR* (*red signals*) and for the centromere of chromosome 7 (*green signals*) in the indicated cell lines. PC-9 and Ma-1 cells manifest an *EGFR*/chromosome copy number ratio of ≥2, whereas KT-2 and KT-4 cells manifest *EGFR* clusters. H1975 and H1650 cells are negative for *EGFR* amplification.

Results

Effect of gefitinib on the growth of NSCLC cell lines. We first examined the effect of the EGFR-TKI gefitinib on the growth of 16 NSCLC cell lines, eight of which (KT-2, KT-4, Ma-1, Ma-25, Ma-31, Ma-34, Ma-45, and Ma-53) were established from Japanese NSCLC patients for the present study. The IC_{50} values for gefitinib chemosensitivity ranged from 0.07 to 12.46 μmol/L (a 178-fold difference; Table 1).

Four cell lines (PC-9, KT-2, KT-4, and Ma-1) were relatively sensitive to gefitinib with IC_{50} values between 0.07 and 2.34 μmol/L, whereas the remaining 12 lines were considered resistant to gefitinib (IC_{50} > 6 μmol/L). No relation was apparent between sensitivity to gefitinib and histologic subtype of NSCLC for this panel of cell lines (Table 1).

***EGFR* mutation and amplification in NSCLC cell lines.** We screened the 16 NSCLC cell lines for the presence of *EGFR* mutations in exons 18 to 21, which encode the catalytic domain of the receptor. As previously described (36–39), PC-9, H1650, and H1975 cell lines were found to harbor *EGFR* mutations [del(E746-A750) in PC-9 and H1650 and both L858R and T790M in H1975]. Furthermore, we detected *EGFR* mutations in three of the newly established cell lines (Ma-1, KT-2, and KT-4). Ma-1 cells, which were isolated from a female ex smoker with adenocarcinoma (>30 years of age), were found to harbor a small deletion within exon 19 [del(E746-A750); Fig. 1*A*; Table 1]. Both KT-2 cells [derived from a male ex smoker with adenocarcinoma (>30 years of age)] and KT-4 cells (derived from a male nonsmoker with large cell carcinoma) harbor a point mutation (L858R) in exon 21 (Fig. 1*B*; Table 1). Four of these six NSCLC cell lines with *EGFR* mutations (PC-9, Ma-1, KT-2, and KT-4) are sensitive to gefitinib (Table 1), consistent with clinical observations (15–17, 20, 22).

We next examined the 16 NSCLC cell lines for the presence of *EGFR* amplification by FISH analysis with a probe specific for *EGFR* and a control probe for the centromere of chromosome 7. Four (PC-9, Ma-1, KT-2, and KT-4) of the 16 cell lines, all of which harbor *EGFR* mutations, were found to be positive for *EGFR* amplification (Fig. 2; Table 1). PC-9 and Ma-1 cell lines, both of which harbor the same exon 19 deletion, showed an *EGFR*/chromosome copy number ratio of ≥2, whereas KT-2 and KT-4, both of which harbor the L858R mutation in exon 21, showed a clustered unbalanced gain of *EGFR* copy number (Fig. 2). The four cell lines that manifested both *EGFR* mutation and amplification were sensitive to gefitinib (Table 1). The *EGFR* mutant cell lines H1650 and H1975 showed no evidence of *EGFR* amplification (Fig. 2), and both of these lines were relatively resistant to gefitinib (Table 1). None of the cell lines negative for *EGFR* mutations manifested *EGFR* amplification (Table 1), suggesting that *EGFR* mutation is closely associated with *EGFR* amplification ($P < 0.05$, χ^2 test).

EGFR expression in NSCLC cell lines. We examined the basal abundance of EGFR in *EGFR* wild-type and mutant NSCLC cell lines by immunoblot analysis. The amount of EGFR in the cell lines PC-9, Ma-1, KT-2, and KT-4, all of which manifest *EGFR* amplification and *EGFR* mutation, was increased compared with that in *EGFR* wild-type cell lines (A549 and H1299) or *EGFR* mutant cell lines negative for *EGFR* amplification (H1975 and H1650; Fig. 3). These results, thus, reveal a close relation between increased EGFR expression and *EGFR* amplification in this panel of NSCLC cell lines, consistent with the results of previous analyses of NSCLC tissue specimens (6, 7).

EGFR phosphorylation in NSCLC cell lines. We examined tyrosine phosphorylation of endogenous EGFRs in NSCLC cell lines by immunoblot analysis with phosphorylation site–specific antibodies. In cells (A549) that express only wild-type EGFR, phosphorylation of the receptor at Y845, Y1068, or Y1173 was undetectable in the absence of EGF but was markedly induced on

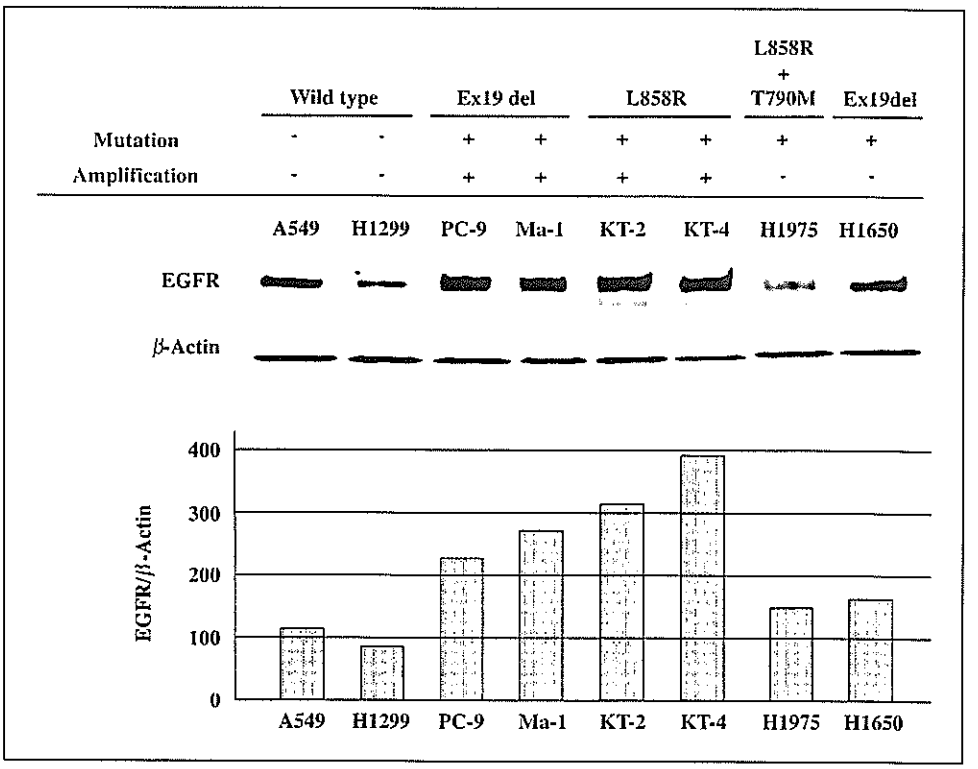

Figure 3. EGFR expression in NSCLC cell lines. Lysates (40 μg of protein) of NSCLC cell lines positive or negative for *EGFR* mutation or amplification, as indicated, were subjected to immunoblot analysis with antibodies to EGFR and to β-actin (*top*). The abundance of EGFR relative to that of β-actin was determined by densitometry (*bottom*). Representative of three independent experiments.

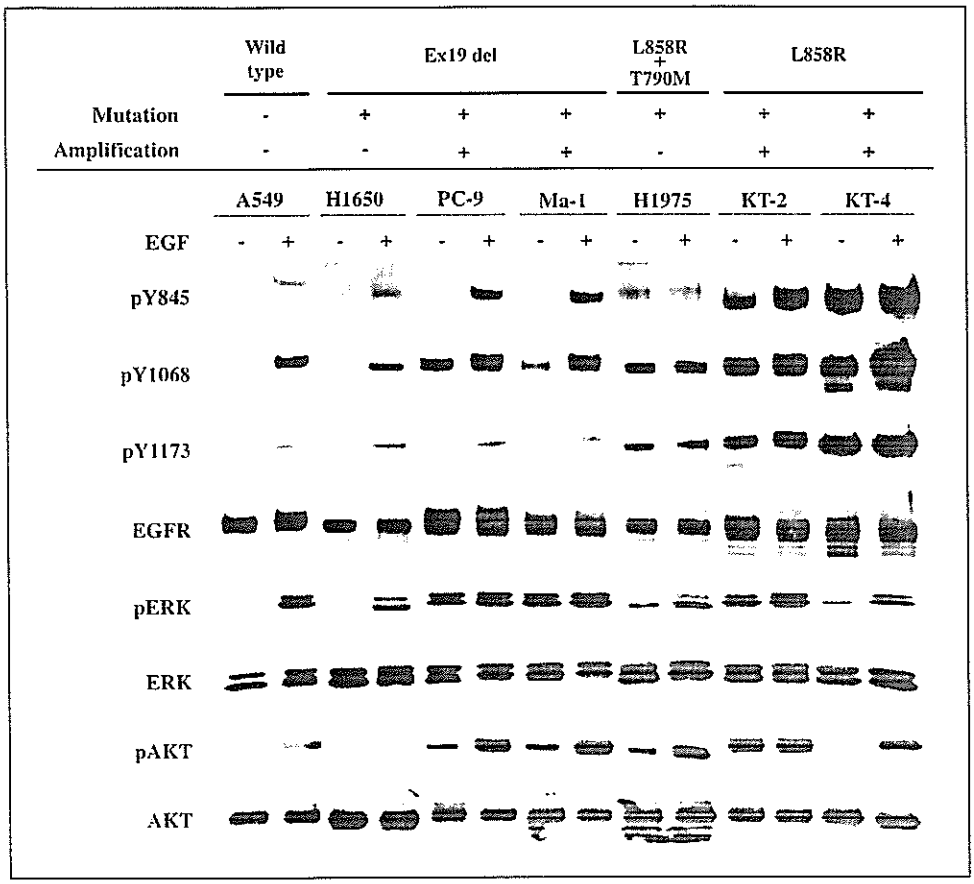

Figure 4. Phosphorylation of EGFR and downstream signaling molecules in NSCLC cell lines. Serum-deprived cells were incubated for 15 min in the absence or presence of EGF (100 ng/mL), after which cell lysates (40 μg of protein) were subjected to immunoblot analysis with antibodies to phosphorylated forms of EGFR (*pEGFR*), ERK (*pERK*), or AKT (*pAKT*) as well as antibodies to all forms of the corresponding proteins, as indicated. Representative of three independent experiments.

exposure of the cells to this growth factor (Fig. 4). Similar results were obtained with H1650 cells, which are positive for the deletion in exon 19 of *EGFR* but negative for *EGFR* amplification. In contrast, PC-9 and Ma-1 cells, which are positive for both the exon 19 deletion and *EGFR* amplification, manifested an increased basal level of EGFR phosphorylation at Y1068, indicative of constitutive activation of the EGFR tyrosine kinase. Exposure of PC-9 or Ma-1 cells to EGF induced EGFR phosphorylation at Y845 and Y1173, showing that the mutant receptors remain sensitive to ligand stimulation. Furthermore, the cell lines (H1975, KT-2, and KT-4) with the L858R point mutation manifested an increased basal level of EGFR phosphorylation at Y845, Y1068, and Y1173, and the extent of phosphorylation at these residues was increased only slightly by treatment of the cells with EGF, indicative of constitutive activation of the EGFR tyrosine kinase. These results thus showed that endogenous *EGFR* mutations result in constitutive receptor activation, and that the patterns of tyrosine phosphorylation of EGFR differ between the two most common types of *EGFR* mutant.

Phosphorylation of signaling molecules downstream of EGFR in NSCLC cell lines. Given that constitutive activation of EGFR was detected in NSCLC cell lines with endogenous *EGFR* mutations, we examined whether signaling molecules that act downstream of the receptor are also constitutively activated in these cell lines. We first examined the basal levels of phosphorylation of AKT and ERK, both of which mediate the oncogenic effects of EGFR. Immunoblot analysis with antibodies to phosphorylated forms of AKT or ERK revealed that these molecules are indeed constitutively activated in the *EGFR* mutant lines (PC-9, Ma-1, H1975, KT-2, and KT-4) that manifest constitutive activation of EGFR, although the extent of phosphorylation varied (Fig. 4). The increased levels of AKT and ERK phosphorylation in these mutant cell lines are consistent with the increased level of EGFR phosphorylation on Y1068, which serves as the docking site for phosphatidylinositol 3-kinase and growth factor receptor binding protein 2, molecules that mediate the activation of AKT and the Ras-ERK pathway, respectively (2, 40). We next examined whether the differences in the pattern of constitutive tyrosine phosphorylation of EGFR apparent between NSCLC cell lines harboring the exon 19 deletion and those with the L858R mutation in exon 21 are associated with distinct alterations in downstream signaling pathways. Given that Y1173, a major docking site of EGFR for the adapter protein Shc (2, 40, 41), is constitutively phosphorylated in cells with the L858R mutation but not in those with the exon 19 deletion, we compared Shc phosphorylation between cell lines with these two types of *EGFR* mutation. Ligand-independent tyrosine phosphorylation of the 52- and 46-kDa isoforms of Shc was apparent in cell lines with either type of *EGFR* mutation (Fig. 5). However, cell lines (KT-2 and KT-4) that harbor the L858R mutation exhibited a markedly greater basal level of phosphorylation of the 66-kDa isoform of Shc than did those (PC-9 and Ma-1) that harbor the exon 19 deletion or those (A549) that harbor only wild-type *EGFR*. These data suggest that the constitutively active mutant forms of *EGFR* induce selective activation of downstream effectors as a result of differential patterns of receptor autophosphorylation.

Ligand-independent dimerization and activation of *EGFR* mutants. Evidence suggests that EGFR ligands, including EGF and TGF-α, secreted by tumor cells themselves might be responsible for activation of mutant receptors in an autocrine loop (29, 42). To investigate whether EGFR is constitutively activated as a result of such an autocrine mechanism in *EGFR* mutant NSCLC cell lines, we treated the cells with a combination of three neutralizing antibodies (anti-EGF, anti–TGF-α, and anti-EGFR) for 3 h and then examined the effect of EGF on EGFR phosphorylation. The ligand-dependent activation of EGFR in A549 cells (which express only wild-type *EGFR*) was blocked by such antibody treatment (Fig. 6*A*). In contrast, treatment of the *EGFR* mutant cell lines PC-9 or KT-4 with the neutralizing antibodies failed to inhibit the constitutive phosphorylation of EGFR on Y1068. These observations suggest that the constitutive phosphorylation of the mutant receptors is not attributable to autocrine stimulation, although we are not able to exclude a possible role for other EGFR ligands.

Ligand-induced EGFR dimerization is responsible for activation of the receptor tyrosine kinase (4, 5). To determine whether mutant receptors are constitutively dimerized, we treated *EGFR* wild-type or mutant cell lines with a cross-linking agent before immunoblot analysis with antibodies to EGFR. Whereas ligand-induced dimerization of wild-type *EGFR* was observed in A549 cells, receptor dimerization in PC-9 and KT-4 cells, which express mutant receptors, was apparent in the absence of ligand and was not increased substantially by exposure of the cells to EGF (Fig. 6*B*). These data indicate that ligand-independent receptor dimerization is responsible for the constitutive activation of the mutant forms of *EGFR*.

Discussion

The discovery of somatic mutations in the tyrosine kinase domain of EGFR and of their association with a high response rate to EGFR-TKIs has had a substantial effect on the treatment of advanced NSCLC (15–17, 20, 22). Asian patients with NSCLC seem to have a higher prevalence of these mutations, ranging from 20% to 40% (18, 20, 21, 43–45). We have now identified *EGFR* mutations in three of eight newly established cell lines from Japanese patients with advanced NSCLC. Characterization of these eight new cell lines and eight previously established NSCLC lines revealed that, consistent with previous observations (29, 31, 36), those cell lines that harbor *EGFR* mutations are more likely to be sensitive to gefitinib than are those without such mutations. Not all *EGFR* mutant cell lines (e.g., H1650 and H1975) are sensitive to this EGFR-TKI, however, suggesting the existence of additional determinants of gefitinib sensitivity. In addition to the L858R mutation in exon 21 of *EGFR*, H1975 cells contain the T790M mutation in exon 20, which has been shown to confer resistance to EGFR-TKIs (38, 39). H1650 cells, which do not harbor mutations in *EGFR* other than the exon 19 deletion, manifest loss of the tumor suppressor phosphatase and tensin homologue deleted on chromosome 10 (37), which may result in resistance to EGFR-TKIs. *EGFR* amplification in NSCLC cells has also been shown to correlate with a better response to gefitinib (22, 25–27). Given that little is known of the relation between *EGFR* mutation and amplification in NSCLC, we examined the 16 NSCLC cell lines used in this study for *EGFR* amplification by FISH. Four of the six cell lines with *EGFR* mutations were found to be positive for gene amplification, whereas none of the 10 mutation-negative cell lines manifested *EGFR* amplification. This finding thus suggests that *EGFR* mutation and amplification are linked. Cappuzzo et al. showed that 6 of 9 (67%) NSCLC patients with *EGFR* amplification also had *EGFR* mutations (25). Furthermore, Takano et al. sequenced *EGFR* and determined the *EGFR* copy number by real-time PCR analysis for the tumors of 66 NSCLC patients (22); all of the patients with a high *EGFR* copy number (≥6.0 per cell) also had *EGFR* mutations. Moreover, PCR analysis revealed selective amplification of the mutant *EGFR* alleles in the patients with a high *EGFR* copy number. Our sequencing electrophoretograms for the *EGFR* mutant cell lines positive for *EGFR* amplification also revealed that the mutant signals were dominant, and the wild-type sequence was barely detectable (Fig. 1), indicative of selective amplification of the mutant alleles. We used the recently proposed definition of *EGFR* amplification as determined by FISH (25, 27) and found that the pattern of gene amplification seemed to be dependent on the

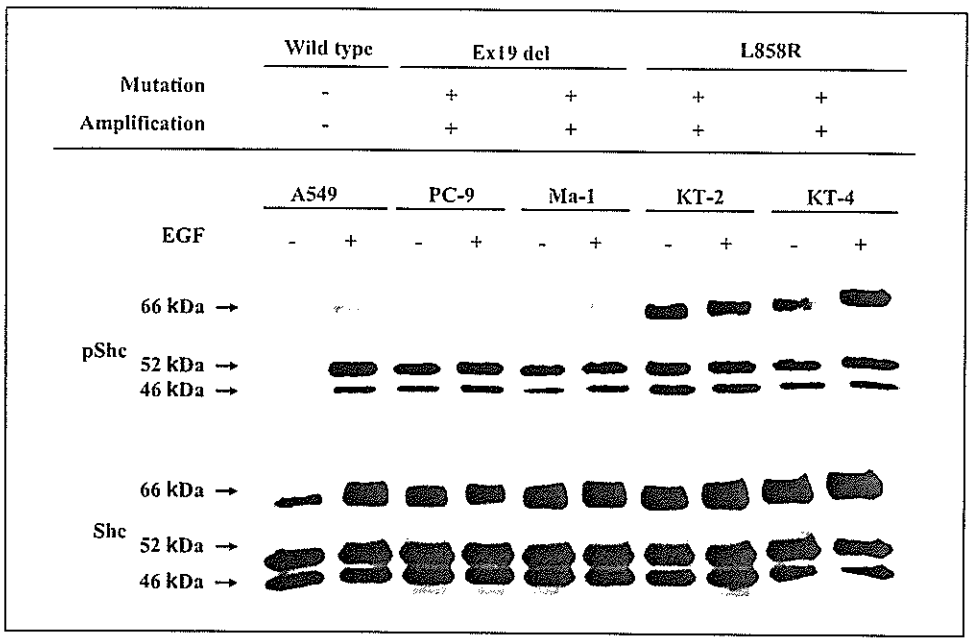

Figure 5. Phosphorylation of Shc in NSCLC cell lines. Serum-deprived cells were incubated for 15 min in the absence or presence of EGF (100 ng/mL), after which cell lysates (40 μg of protein) were subjected to immunoblot analysis with antibodies to phosphorylated Shc (*pShc*) or total Shc. Representative of three independent experiments.

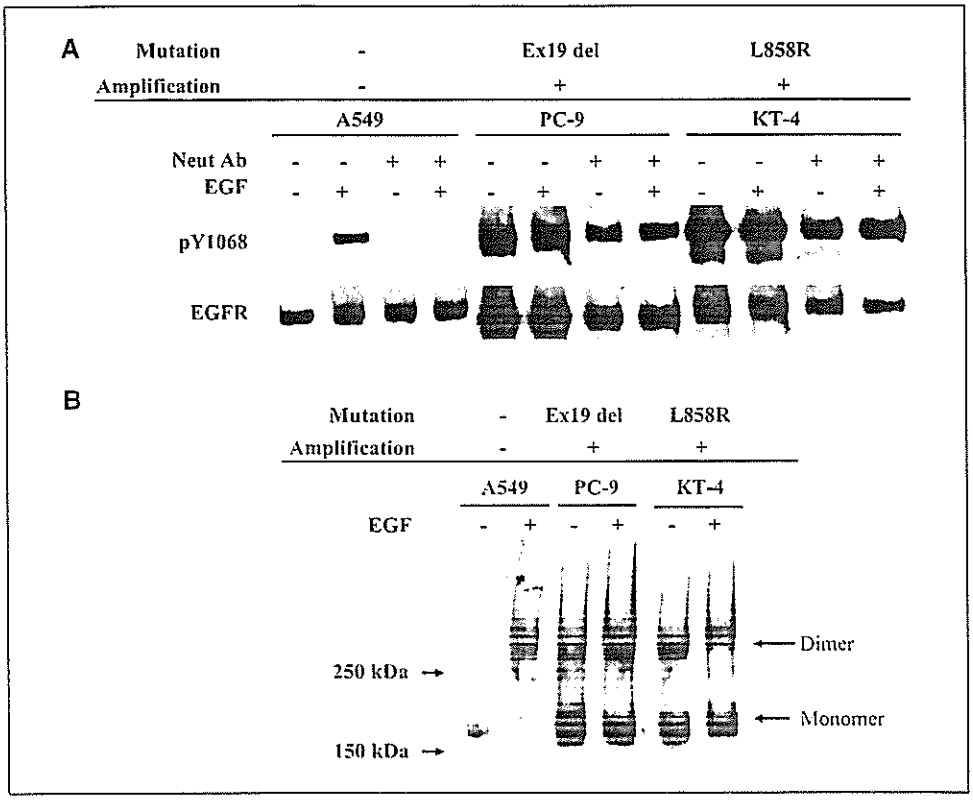

Figure 6. Mechanism of constitutive activation of EGFR in NSCLC cell lines. *A*, effect of neutralizing antibodies (*Neut Ab*) on EGFR phosphorylation. Serum-deprived NSCLC cells (A549, PC-9, or KT-4) were incubated for 3 h with a combination of neutralizing antibodies to EGF, TGF-α, and EGFR and then for 15 min in the additional absence or presence of EGF (100 ng/mL). Cell lysates were then prepared and subjected to immunoblot analysis with antibodies to the Y1068-phosphorylated form of EGFR or to total EGFR. *B*, EGFR dimerization. Serum-deprived cells were incubated for 15 min in the absence or presence of EGF (100 ng/mL), exposed to a chemical cross-linker, lysed, and subjected to immunoblot analysis with antibodies to EGFR. Representative of three independent experiments.

type of *EGFR* mutation; gene clusters were observed in cells with the L858R mutation in exon 21, whereas an *EGFR*/chromosome copy number ratio of ≥2 was detected in those with the small deletion [del(E746-A750)] in exon 19. Together, these data support the notion that *EGFR* mutation and amplification may be co-selected for during the growth of NSCLC cells. The four cell lines (PC-9, Ma-1, KT-2, and KT-4) positive for both *EGFR* mutation and amplification were sensitive to gefitinib, suggesting that *EGFR* amplification may increase sensitivity to gefitinib in *EGFR* mutant cells.

Previous biochemical studies of cells transiently transfected with vectors for wild-type or mutant forms of EGFR suggested that *EGFR* mutations increase EGF-dependent receptor activation (15, 30). Infection of NIH 3T3 cells with a retrovirus encoding *EGFR* mutants showed that the mutant receptors are constitutively activated and able to induce cell transformation in the absence of exogenous EGF (32). We examined the activation status of endogenous EGFRs in the six NSCLC cell lines that harbor *EGFR* mutations. The H1650, PC-9, and Ma-1 cell lines, all of which harbor the same exon 19 deletion, showed different patterns of EGFR autophosphorylation in the COOH-terminal region of the protein. EGFR autophosphorylation was ligand dependent in H1650 cells, which are negative for *EGFR* amplification, whereas Y1068 (but not Y845 and Y1173) was constitutively phosphorylated in PC-9 and Ma-1 cells, both of which manifest *EGFR* amplification. These results suggest that both *EGFR* mutation and amplification may be required for constitutive activation of EGFR in NSCLC cells that harbor the exon 19 deletion. In contrast, NSCLC cell lines (H1975, KT-2, and KT-4) that harbor the L858R mutation exhibited constitutive phosphorylation of EGFR at Y845, Y1068, and Y1173, regardless of the absence or presence of *EGFR* amplification. It is thought that *EGFR* mutations result in repositioning of critical residues surrounding the ATP-binding cleft of the tyrosine kinase domain of the receptor and thereby stabilize the interactions with ATP and EGF-TKIs, leading to increased tyrosine kinase activity and EGFR-TKI sensitivity (15, 23, 24). The differential activation of *EGFR* mutants observed in the present study may result from distinct conformational changes within the catalytic pocket caused by the different types of *EGFR* mutation. NSCLC patients with exon 19 deletions were recently shown to manifest longer overall survival than did those with the exon 21 point mutation after treatment with EGFR-TKIs, supporting the notion that the two major types of mutant receptors have different biological properties (46, 47).

Ligand-induced receptor dimerization underlies the activation of receptor tyrosine kinases (4, 5). Chemical cross-linking revealed that EGF binding to EGFR induced receptor dimerization in A549 cells, which express only the wild-type form of the receptor. In contrast, endogenous EGFRs in NSCLC cells harboring either the exon 19 deletion or the point mutation in exon 21 of *EGFR* were found to dimerize in the absence of ligand, suggesting that the constitutive activation of the mutant receptors is attributable to ligand-independent dimerization. EGFR dimerization was shown to be induced by interaction of quinazolines with the ATP-binding site of the receptor in the absence of ligand binding, suggesting that a change in conformation around the ATP-binding pocket of EGFR is sufficient for receptor dimerization (35). Conformational changes induced by *EGFR* mutations may therefore also trigger EGFR dimerization in *EGFR* mutant cells.

In conclusion, we have found that *EGFR* mutation is closely associated with *EGFR* amplification in NSCLC cell lines. Endogenous EGFRs expressed in NSCLC cells positive for both *EGFR* mutation and amplification are constitutively activated as a result

of ligand-independent dimerization. Cells with the two most common types of *EGFR* mutation also manifest different patterns of EGFR autophosphorylation. Prospective studies are required to determine the potential for exploitation of these *EGFR* alterations in the treatment of advanced NSCLC.

Acknowledgments

Received 9/12/2006; revised 10/30/2006; accepted 12/10/2006.

The costs of publication of this article were defrayed in part by the payment of page charges. This article must therefore be hereby marked *advertisement* in accordance with 18 U.S.C. Section 1734 solely to indicate this fact.

We thank Takeko Wada, Erina Hatashita, and Yuki Yamada for technical assistance.

References

1. Wang Y, Minoshima S, Shimizu N. Precise mapping of the EGF receptor gene on the human chromosome 7p12 using an improved FISH technique. Jpn J Hum Genet 1993;38:399–406.
2. Jorissen RN, Walker F, Pouliot N, Garrett TP, Ward CW, Burgess AW. Epidermal growth factor receptor: mechanisms of activation and signalling. Exp Cell Res 2003; 284:31–53.
3. Hynes NE, Lane HA. ERBB receptors and cancer: the complexity of targeted inhibitors. Nat Rev Cancer 2005; 5:341–54.
4. Ogiso H, Ishitani R, Nureki O, et al. Crystal structure of the complex of human epidermal growth factor and receptor extracellular domains. Cell 2002;110:775–87.
5. Schlessinger J. Ligand-induced, receptor-mediated dimerization and activation of EGF receptor. Cell 2002;110:669–72.
6. Hirsch FR, Varella-Garcia M, Bunn PA, Jr., et al. Epidermal growth factor receptor in non-small-cell lung carcinomas: correlation between gene copy number and protein expression and impact on prognosis. J Clin Oncol 2003;21:3798–807.
7. Suzuki S, Dobashi Y, Sakurai H, Nishikawa K, Hanawa M, Ooi A. Protein overexpression and gene amplification of epidermal growth factor receptor in nonsmall cell lung carcinomas. An immunohistochemical and fluorescence *in situ* hybridization study. Cancer 2005;103: 1265–73.
8. Shepherd FA, Rodrigues Pereira J, Ciuleanu T, et al. Erlotinib in previously treated non-small-cell lung cancer. N Engl J Med 2005;353:123–32.
9. Thatcher N, Chang A, Parikh P, et al. Gefitinib plus best supportive care in previously treated patients with refractory advanced non-small-cell lung cancer: results from a randomised, placebo-controlled, multicentre study (Iressa Survival Evaluation in Lung Cancer). Lancet 2005;366:1527–37.
10. Fukuoka M, Yano S, Giaccone G, et al. Multi-institutional randomized phase II trial of gefitinib for previously treated patients with advanced non-small-cell lung cancer (the IDEAL 1 trial). J Clin Oncol 2003;21: 2237–46.
11. Kaneda H, Tamura K, Kurata T, Uejima H, Nakagawa K, Fukuoka M. Retrospective analysis of the predictive factors associated with the response and survival benefit of gefitinib in patients with advanced non-small-cell lung cancer. Lung Cancer 2004;46:247–54.
12. Takano T, Ohe Y, Kusumoto M, et al. Risk factors for interstitial lung disease and predictive factors for tumor response in patients with advanced non-small cell lung cancer treated with gefitinib. Lung Cancer 2004;45:93–104.
13. Tamura K, Fukuoka M. Gefitinib in non-small cell lung cancer. Expert Opin Pharmacother 2005;6:985–93.
14. Ando M, Okamoto I, Yamamoto N, et al. Predictive factors for interstitial lung disease, antitumor response, and survival in non-small-cell lung cancer patients treated with gefitinib. J Clin Oncol 2006;24:2549–56.
15. Lynch TJ, Bell DW, Sordella R, et al. Activating mutations in the epidermal growth factor receptor underlying responsiveness of non-small-cell lung cancer to gefitinib. N Engl J Med 2004;350:2129–39.
16. Paez JG, Janne PA, Lee JC, et al. EGFR mutations in lung cancer: correlation with clinical response to gefitinib therapy. Science 2004;304:1497–500.
17. Pao W, Miller V, Zakowski M, et al. EGF receptor gene mutations are common in lung cancers from "never smokers" and are associated with sensitivity of tumors to gefitinib and erlotinib. Proc Natl Acad Sci U S A 2004; 101:13306–11.
18. Kosaka T, Yatabe Y, Endoh H, Kuwano H, Takahashi T, Mitsudomi T. Mutations of the epidermal growth factor receptor gene in lung cancer: biological and clinical implications. Cancer Res 2004; 64:8919–23.
19. Han SW, Kim TY, Hwang PG, et al. Predictive and prognostic impact of epidermal growth factor receptor mutation in non-small-cell lung cancer patients treated with gefitinib. J Clin Oncol 2005;23:2493–501.
20. Mitsudomi T, Kosaka T, Endoh H, et al. Mutations of the epidermal growth factor receptor gene predict prolonged survival after gefitinib treatment in patients with non-small-cell lung cancer with postoperative recurrence. J Clin Oncol 2005;23:2513–20.
21. Tokumo M, Toyooka S, Kiura K, et al. The relationship between epidermal growth factor receptor mutations and clinicopathologic features in non-small cell lung cancers. Clin Cancer Res 2005;11:1167–73.
22. Takano T, Ohe Y, Sakamoto H, et al. Epidermal growth factor receptor gene mutations and increased copy numbers predict gefitinib sensitivity in patients with recurrent non-small-cell lung cancer. J Clin Oncol 2005;23:6829–37.
23. Gazdar AF, Shigematsu H, Herz J, Minna JD. Mutations and addiction to EGFR: the Achilles 'heal' of lung cancers? Trends Mol Med 2004;10:481–6.
24. Shigematsu H, Gazdar AF. Somatic mutations of epidermal growth factor receptor signaling pathway in lung cancers. Int J Cancer 2006;118:257–62.
25. Cappuzzo F, Hirsch FR, Rossi E, et al. Epidermal growth factor receptor gene and protein and gefitinib sensitivity in non-small-cell lung cancer. J Natl Cancer Inst 2005;97:643–55.
26. Hirsch FR, Varella-Garcia M, McCoy J, et al. Increased epidermal growth factor receptor gene copy number detected by fluorescence *in situ* hybridization associates with increased sensitivity to gefitinib in patients with bronchioloalveolar carcinoma subtypes: a Southwest Oncology Group Study. J Clin Oncol 2005;23:6838–45.
27. Tsao MS, Sakurada A, Cutz JC, et al. Erlotinib in lung cancer: molecular and clinical predictors of outcome. N Engl J Med 2005;353:133–44.
28. Ishikawa N, Daigo Y, Takano A, et al. Increases of amphiregulin and transforming growth factor-α in serum as predictors of poor response to gefitinib among patients with advanced non-small cell lung cancers. Cancer Res 2005;65:9176–84.
29. Tracy S, Mukohara T, Hansen M, Meyerson M, Johnson BE, Janne PA. Gefitinib induces apoptosis in the EGFRL858R non-small-cell lung cancer cell line H3255. Cancer Res 2004;64:7241–4.
30. Sordella R, Bell DW, Haber DA, Settleman J. Gefitinib-sensitizing EGFR mutations in lung cancer activate anti-apoptotic pathways. Science 2004;305:1163–7.
31. Amann J, Kalyankrishna S, Massion PP, et al. Aberrant epidermal growth factor receptor signaling and enhanced sensitivity to EGFR inhibitors in lung cancer. Cancer Res 2005;65:226–35.
32. Greulich H, Chen TH, Feng W, et al. Oncogenic transformation by inhibitor-sensitive and -resistant EGFR mutants. PLoS Med 2005;2:1167–76.
33. Yonesaka K, Tamura K, Kurata T, et al. Small interfering RNA targeting survivin sensitizes lung cancer cell with mutant p53 to Adriamycin. Int J Cancer 2006; 118:812–20.
34. Koizumi F, Shimoyama T, Taguchi F, Saijo N, Nishio K. Establishment of a human non-small cell lung cancer cell line resistant to gefitinib. Int J Cancer 2005;116:36–44.
35. Arteaga CL, Ramsey TT, Shawver LK, Guyer CA. Unliganded epidermal growth factor receptor dimerization induced by direct interaction of quinazolines with the ATP binding site. J Biol Chem 1997;272:23247–54.
36. Mukohara T, Engelman JA, Hanna NH, et al. Differential effects of gefitinib and cetuximab on non-small-cell lung cancers bearing epidermal growth factor receptor mutations. J Natl Cancer Inst 2005;97:1185–94.
37. Janmaat ML, Rodriguez JA, Gallegos-Ruiz M, Kruyt FA, Giaccone G. Enhanced cytotoxicity induced by gefitinib and specific inhibitors of the Ras or phosphatidyl inositol-3 kinase pathways in non-small cell lung cancer cells. Int J Cancer 2006;118:209–14.
38. Pao W, Miller VA, Politi KA, et al. Acquired resistance of lung adenocarcinomas to gefitinib or erlotinib is associated with a second mutation in the EGFR kinase domain. PLoS Med 2005;2:225–35.
39. Kobayashi S, Ji H, Yuza Y, et al. An alternative inhibitor overcomes resistance caused by a mutation of the epidermal growth factor receptor. Cancer Res 2005; 65:7096–101.
40. Olayioye MA, Neve RM, Lane HA, Hynes NE. The ErbB signaling network: receptor heterodimerization in development and cancer. EMBO J 2000;19:3159–67.
41. Okabayashi Y, Kid Y, Okutani T, Sugimoto Y, Sakaguchi K, Kasuga M. Tyrosines 1148 and 1173 of activated human epidermal growth factor receptors are binding sites of Shc in intact cells. J Biol Chem 1994;269: 18674–8.
42. Riemenschneider MJ, Bell DW, Haber DA, Louis DN. Pulmonary adenocarcinomas with mutant epidermal growth factor receptors. N Engl J Med 2005;352:1724–5.
43. Shigematsu H, Lin L, Takahashi T, et al. Clinical and biological features associated with epidermal growth factor receptor gene mutations in lung cancers. J Natl Cancer Inst 2005;97:339–46.
44. Calvo E, Baselga J. Ethnic differences in response to epidermal growth factor receptor tyrosine kinase inhibitors. J Clin Oncol 2006;24:2158–63.
45. Sugio K, Uramoto H, Ono K, et al. Mutations within the tyrosine kinase domain of EGFR gene specifically occur in lung adenocarcinoma patients with a low exposure of tobacco smoking. Br J Cancer 2006;94:896–903.
46. Riely GJ, Pao W, Pham D, et al. Clinical course of patients with non-small cell lung cancer and epidermal growth factor receptor exon 19 and exon 21 mutations treated with gefitinib or erlotinib. Clin Cancer Res 2006; 12:839–44.
47. Jackman DM, Yeap BY, Sequist LV, et al. Exon 19 deletion mutations of epidermal growth factor receptor are associated with prolonged survival in non-small cell lung cancer patients treated with gefitinib or erlotinib. Clin Cancer Res 2006;12:3908–14.

VOLUME 24 · NUMBER 33 · NOVEMBER 20 2006

JOURNAL OF CLINICAL ONCOLOGY

ORIGINAL REPORT

Phase II Study of Etoposide and Cisplatin With Concurrent Twice-Daily Thoracic Radiotherapy Followed by Irinotecan and Cisplatin in Patients With Limited-Disease Small-Cell Lung Cancer: West Japan Thoracic Oncology Group 9902

Hiroshi Saito, Yoshiki Takada, Yukito Ichinose, Kenji Eguchi, Shinzoh Kudoh, Kaoru Matsui, Kazuhiko Nakagawa, Minoru Takada, Shunichi Negoro, Kenji Tamura, Masahiko Ando, Takuhito Tada, and Masahiro Fukuoka

From the Department of Respiratory Medicine, Aichi Cancer Center Aichi Hospital, Okazaki, Aichi; Departments of Thoracic Oncology and Respiratory Medicine, Hyogo Medical Center for Adults, Akashi, Hyogo; Department of Thoracic Oncology, National Hospital Organization Kyushu Cancer Center, Fukuoka; Department of Internal Medicine, National Hospital Organization Shikoku Cancer Center, Matsuyama, Ehime; Department of Respiratory Medicine, Osaka City University Hospital; Department of Thoracic Malignancy, Osaka Prefectural Medical Center for Respiratory and Allergic Diseases, Habikino; Department of Medical Oncology, Kinki University School of Medicine, Osakasayama; Department of Pulmonary Medicine, Rinku General Medical Center, Izumisano; Department of Radiology, Osaka Prefectural Medical Center for Respiratory and Allergic Diseases, Habikino, Osaka; Department of Medical Oncology, Kinki University School of Medicine, Nara Hospital, Ikoma, Nara; and the Health Service, Kyoto University, Kyoto, Japan.

Submitted May 3, 2006; accepted September 7, 2006.

Presented in part at the 39th Annual Meeting of the American Society of Clinical Oncology, May 31-June 3, 2003, Chicago, IL, and the 40th Annual Meeting of the American Society of Clinical Oncology, June 5-8, 2004, New Orleans, LA.

Authors' disclosures of potential conflicts of interest and author contributions are found at the end of this article.

Address reprint requests to Hiroshi Saito, MD, Department of Respiratory Medicine, Aichi Cancer Center Aichi Hospital, 18 Kuriyado Kake-machi, Okazaki Aichi 444-0011, Japan; e-mail: hsaitot@sun-inet.or.jp.

0732-183X/06/2433-5247/$20.00

DOI: 10.1200/JCO.2006.07.1605

A B S T R A C T

Purpose
We initially conducted a randomized phase II study to compare irinotecan and cisplatin (IP) versus irinotecan, cisplatin, and etoposide (IPE) after etoposide and cisplatin (EP) with concurrent twice-daily thoracic radiotherapy (TRT) in limited-disease small-cell lung cancer (LD-SCLC). We amended the protocol to evaluate IP after EP with concurrent twice-daily TRT in a single-arm phase II study because of an unacceptable toxicity in IPE.

Patients and Methods
Previously untreated patients with LD-SCLC were treated intravenously with etoposide 100 mg/m^2 on days 1 through 3 and cisplatin 80 mg/m^2 on day 1 with concurrent twice-daily TRT (1.5 Gy per fraction, a total dose of 45 Gy) beginning on day 2 followed by three cycles of irinotecan 60 mg/m^2 on days 1, 8, and 15 and cisplatin 60 mg/m^2 on day 1 of a 4-week cycle.

Results
Of the 51 patients enrolled, 49 patients were assessable for response and toxicity. The overall response rate and complete response rate were 88% and 41%, respectively. The median survival time for all patients was 23 months. The 2-year and 3-year survival rates were 49% and 29.7%, respectively. The median progression-free survival was 11.8 months. The major toxicities observed were neutropenia (grade 4, 84%), febrile neutropenia (grade 3, 31%), infection (grade 3 to 4, 33%), electrolytes imbalance (grade 3 to 4, 20%), and diarrhea (grade 3 to 4, 14%).

Conclusion
EP with concurrent twice-daily TRT followed by the consolidation of IP appears to be an active regimen which deserves further phase III testing in patients with LD-SCLC.

J Clin Oncol 24:5247-5252. © 2006 by American Society of Clinical Oncology

Introduction

Small-cell lung cancer (SCLC), which accounts for approximately 15% of all lung cancer cases, is clinically categorized as the two stages, limited disease and extensive disease. Two meta-analyses have shown the combined modality of chemotherapy and thoracic radiotherapy (TRT) to improve the survival of patients with limited-disease (LD-) SCLC in comparison to chemotherapy alone.[1,2] The schedule, dose, and fractionation of TRT have previously been examined in patients with LD-SCLC in several randomized controlled studies.[3-7] On the basis of the results of these studies, etoposide and cisplatin (EP) with concurrent twice-daily TRT is currently a standard care for the treatment for LD-SCLC. However, the 5-year survival rate is less than 30%, and most patients experience a relapse of the primary tumor or distant metastasis.[3-6] To further improve the therapeutic efficacy, one approach is to develop a new chemoradiotherapy regimen incorporating with a novel active agent.

Irinotecan hydrochloride, a camptothecin derivative, is among the most active chemotherapeutic agents against SCLC with a response rate of 37% as a single agent.[8] A randomized phase III study revealed that irinotecan and cisplatin (IP) was superior to EP in patients with extensive-disease SCLC (ED-SCLC).[9] However, the role of IP in the treatment of LD-SCLC remains to be defined. To clarify the role of this combination regimen in LD-SCLC, we initially conducted a randomized phase II study to

compare two consolidation chemotherapy regimens, IP versus irinotecan, cisplatin and etoposide (IPE), after EP with concurrent twice-daily TRT in LD-SCLC.[10] However, EP with concurrent twice-daily TRT followed by IPE was not feasible because of unacceptable toxicity including grade 4 neutropenia (92%), grade 4 diarrhea (25%), grade 4 infection (25%) and one treatment-related death. We therefore amended the protocol to evaluate EP with concurrent twice-daily TRT followed by consolidation therapy with IP in a single-arm phase II study and herein report the results of this study.

PATIENTS AND METHODS

Eligibility Criteria

Patients with histologically or cytologically confirmed LD-SCLC (stage I disease was excluded) were eligible for this study. A limited stage was defined as disease confined to one hemithorax, the mediastinum, and the bilateral supraclavicular area. Cases with a small amount of pleural effusion and a negative cytology were included in the limited-stage group. Other eligibility criteria included the following: no prior chemotherapy or radiotherapy; measurable disease; Eastern Cooperative Oncology Group (ECOG) performance status of 0 to 2; age between 20 and 70 years; life expectancy of at least 3 months; adequate baseline organ function defined as leukocyte count ranging from 4,000 to 12,000/mm^3, hemoglobin concentration of at least 9.5 g/dL, platelet count at least 100,000/mm^3, AST and ALT 2.0× the upper limit of the normal range (ULN) or less, serum total bilirubin 1.5 mg/dL or less, serum creatinine ULN or less, 24-hour creatinine clearance of at least 60 mL/min, and Pao_2 at rest of at least 70 mmHg. The radiation portal should be equal or less than half of one lung.

The patients were ineligible if they had the following criteria: interstitial pneumonitis or pulmonary fibrosis; other respiratory diseases that precluded TRT; malignant pleural effusion or malignant pericardial effusion; active concomitant or a recent (< 3 years) history of any malignancy; uncontrolled angina pectoris, myocardial infarction less than 3 months before the enrollment or congestive heart failure; uncontrolled diabetes mellitus or hypertension; severe infection; intestinal paralysis or obstruction; pregnancy or lactation; or other serious concomitant medical conditions. The study protocol was approved by each institutional review board for clinical use. All patients gave their written informed consent before enrollment.

Study Evaluation

The pretreatment baseline evaluation included a complete medical history and physical examination, a CBC, blood chemistry studies, flexible bronchoscopy, electrocardiography, chest radiography, computed tomography of the chest, computed tomography or ultrasound study of the abdomen, computed tomography or magnetic resonance imaging of the brain, bone scintigraphy and bone marrow aspiration with or without biopsy. A CBC and blood chemistry studies were repeated every week. At the end of the study, all of these studies except for flexible bronchoscopy and bone marrow aspiration were repeated unless the patient had stable or progressive disease.

Treatment Schedule

The patients initially received induction chemoradiotherapy consisting of etoposide 100 mg/m^2 on day 1 through 3 and cisplatin 80 mg/m^2 on day 1 with concurrent twice-daily TRT. After the induction chemoradiotherapy, the patients received three cycles of consolidation chemotherapy consisting of irinotecan 60 mg/m^2 on days 1, 8, and 15 and cisplatin 60 mg/m^2 on days 1. Consolidation chemotherapy was repeated every 4 weeks for three cycles.

The first cycle of consolidation chemotherapy was begun 4 week after the initiation of induction chemoradiotherapy if the leukocyte count was at least 4,000/mm^3; the platelet count was at least 100,000/mm^3; AST and ALT 2.0× ULN or less; serum bilirubin 1.5 mg/dL or less; serum creatinine of ULN or less; the patient did not have fever (≧ 38°C), diarrhea within the past 24 hours, or intestinal paralysis or obstruction; and Pao_2 of at least 70 mmHg. The subsequent cycle of consolidation chemotherapy was repeated if the leukocyte count was at least 3,500/mm^3; the platelet count was at least 100,000/mm^3; AST and ALT 2.0× ULN or less; serum bilirubin 1.5 mg/dL or less; serum creatinine ULN or less; the patient did not have fever (≧ 38°C), diarrhea within the past 24 hours, or intestinal paralysis or obstruction. The use of granulocyte colony-stimulating factor (GCSF) was recommended after day 4. However, its administration was withheld on the day of administration of irinotecan.

TRT was performed with 6 MV or higher photons from a linear accelerator and began on day 2 of the induction chemoradiotherapy. Patients received 1.5 Gy per fraction twice daily with at least a 4-hour interval (preferably a 6-hour interval or more) between each fraction over a 3-week period (a total dose of 45 Gy). A radiation field included the primary tumor, the bilateral mediastinal and ipsilateral hilar lymph nodes with a margin of 1.5 to 2.0 cm. Radiation to the supraclavicular lymph nodes was administered only if they were involved. The inferior border extended 5 cm below the carina or to a level including ipsilateral hilar structures, whichever was lower. After initial irradiation with a dose of 30 Gy, off-cord (ie, the spinal cord was outside the field) oblique boost fields were used. The radiation field in the afternoon was not different from that in the morning. Computed tomography planning was not required and lung density corrections were not performed. Prophylactic cranial irradiation (PCI) was administered to the patients achieving complete response or good partial response with a total dose of 25 Gy in 10 fractions.

Dose Modification

Dose modification based on the toxicity of the induction chemoradiotherapy was not allowed at the time of the first administration of IP. In each cycle of IP, irinotecan on day 8 or 15 was withheld if a leukocyte count of less than 2,000/mm^3 or a platelet count of less than 50,000/mm^3 was determined, or if a patient had fever (≧ 38°C) or grade 2 or higher hepatotoxicity or any diarrhea within the last 24 hours or intestinal paralysis or obstruction. In the second and the third cycle of consolidation chemotherapy, the dose modification was made as follows. If a leukocyte nadir count of less than 1,000/mm^3 or a neutrophil nadir count of less than 500/mm^3 for 3 or more days or if febrile neutropenia developed or if a platelet nadir count of less than 25,000/mm^3 was observed or if grade 2 hepatotoxicity or diarrhea was observed, irinotecan was decreased by 10 mg/m^2 in the subsequent cycle, if grade 2 or lower renal toxicity was observed during the previous course of treatment, only cisplatin decreased by 25%, if grade 3 or higher nonhematologic toxicity (excluding nausea, vomiting, and hair loss) developed, then cisplatin decreased by 25% and irinotecan decreased by 10 mg/m^2 in the following cycle. The patients were removed from the study if the following toxicities were observed: grade 4 diarrhea; grade 3 or higher renal toxicity or creatinine of at least 2.0 mg/dL; grade 3 or higher hepatotoxicity; grade 2 or higher pulmonary toxicity or Pao_2 at rest less than 60 mmHg.

Evaluation

The Response Evaluation Criteria in Solid Tumors (RECIST) were used for the response assessment.[11] Toxicity was evaluated according to the National Cancer Institute–Common Toxicity Criteria (version 2.0). An extramural review was conducted to validate the eligibility of the patients, staging, and response.

Statistical Analysis

The primary end point of this study was the 2-year survival rate. We calculated the sample size based on Fleming's single-stage design of the phase II study.[12] We set a 2-year survival rate of 35% as a baseline survival rate and 20% as the high level of interest with a power of 0.9 at a one-sided significance level of .05, requiring an accrual of 53 eligible patients. The study was initially begun as a randomized phase II study to compare two consolidation arms, namely IP versus IPE after concurrent chemoradiotherapy. Because of the unacceptable toxicity in the triplet regimen, the study was modified to a single-arm phase II study to evaluate IP after EP with concurrent TRT and 11 patients in the IP arm were included in the analysis of this study.

The duration of survival was measured from the day of entry onto the study, and the overall survival curve and progression-free survival curve were calculated according to the method of Kaplan and Meier.[13]